Contract No. and Disclaimer:

This manuscript has been authored by Savannah River Nuclear Solutions, LLC under Contract No. DE-AC09-08SR22470 with the U.S. Department of Energy. The United States Government retains and the publisher, by accepting this article for publication, acknowledges that the United States Government retains a non-exclusive, paid-up, irrevocable, worldwide license to publish or reproduce the published form of this work, or allow others to do so, for United States Government purposes.

International Conference on Mathematics and Computational Methods Applied to Nuclear Science and Engineering (M&C 2011)
Rio de Janeiro, RJ, Brazil, May 8-12, 2011, on CD-ROM, Latin American Section (LAS) / American Nuclear Society (ANS)
ISBN 978-85-63688-00-2

MONTE-CARLO BURNUP CALCULATION UNCERTAINTY QUANTIFICATION AND PROPAGATION DETERMINATION

Matthew R. Sternat and William S. Charlton
Nuclear Security Science and Policy Institute
Texas A&M University – Department of Nuclear Engineering
3473 TAMU
Texas A&M University
College Station, TX 77843-3473
m.sternat@tamu.edu; charlton@ne.tamu.edu

Theodore F. Nichols
Savannah River National Laboratory
Savannah River Nuclear Solutions
Aiken, SC 29803
theodore.nichols@srs.gov

ABSTRACT

MONTEBURNS is a Monte-Carlo depletion routine utilizing MCNP and ORIGEN 2.2. Uncertainties exist in the MCNP transport calculation, but this information is not passed to the depletion calculation in ORIGEN or saved. To quantify this transport uncertainty and determine how it propagates between burnup steps, a statistical analysis of a multiple repeated depletion runs is performed. The reactor model chosen is the Oak Ridge Research Reactor (ORR) in a single assembly, infinite lattice configuration. This model was burned for a 25.5 day cycle broken down into three steps. The output isotopics as well as effective multiplication factor (k-effective) were tabulated and histograms were created at each burnup step using the Scott Method to determine the bin width.

It was expected that the gram quantities and k-effective histograms would produce normally distributed results since they were produced from a Monte-Carlo routine, but some of results do not. The standard deviation at each burnup step was consistent between fission product isotopes as expected, while the uranium isotopes created some unique results. The variation in the quantity of uranium was small enough that, from the reaction rate MCNP tally, round off error occurred producing a set of repeated results with slight variation. Statistical analyses were performed using the χ^2 test against a normal distribution for several isotopes and the k-effective results. While the isotopes failed to reject the null hypothesis of being normally distributed, the χ^2 statistic grew through the steps in the k-effective test. The null hypothesis was rejected in the later steps. These results suggest, for a high accuracy solution, MCNP cell material quantities less than 100 grams and greater kcode parameters are needed to minimize uncertainty propagation and minimize round off effects.

Key Words: MONTEBURNS, Monte-Carlo, uncertainty, propagation, burnup, nuclear forensics.

1. INTRODUCTION

MONTEBURNS is a routine that links the Monte-Carlo Neutral Particle transport code (MCNP) with the Oak Ridge Isotope Generation and Depletion Code (ORIGEN 2.2) for burnup and depletion calculations [1]. In the MCNP steps of the routine, tallies are used to compute the total and six group neutron flux and reaction rates. These are then passed to ORIGEN though text files, along with isotopic information, which will compute the fission products, actinides, and activation products produced for the burnup step using the matrix exponential method [2]. There exists an uncertainty in each MCNP tally which is not passed to ORIGEN or saved. Quantification and an understanding on how these uncertainties propagate between burnup steps and the effect on model output isotopic composition were to be determined.

2. ANALYSIS AND RESULTS

To determine the tally uncertainty's effect on k-effective and the reactor isotopics, the same model was burned 200 times using different MCNP starting random seeds. Each of these will produce three burnup step isotopics and four k-effective calculations. It was expected that these would produce a normal distribution of results. To determine the kcode parameters in the MCNP model, the exact tallies MONTEBURNS creates were run numerous times varying the number of particles until the flux and reaction rate tallies passed all statistical tests. This was performed twice for verification.

2.1. MCNP Model Description

The reactor model used for this analysis was the Oak Ridge Research Reactor (ORR). A single assembly of this reactor was modeled in MCNP in an infinite lattice configuration using periodic boundary conditions in the X and Y dimensions shown in Figure 1.

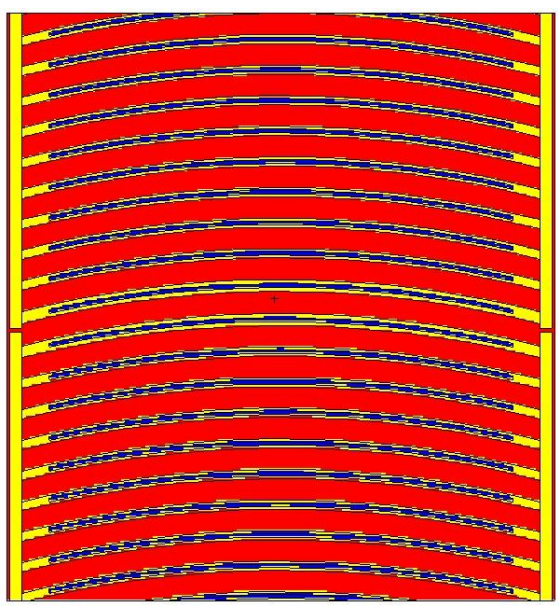

Figure 1. MCNP model of ORR in an infinite lattice configuration.

MTR fuel assemblies possess curved fuel plates which overlap in one dimension. To simulate an infinite lattice, a translation of part of the assembly must be done to preserve the correct assembly pitch. In this model, half of the assembly was translated and burned 200 times with fuel and burnup parameters shown in Table I [3].

Table I. MONTEBURNS fuel and depletion parameters for ORR.

Parameter	Value
^{235}U Enrichment	93%
Material Form	U_3O_8
Other U Isotopes	234, 236, 238
Cladding Material	Al
Side Plate Material	Al
Days Burned [d]	25.5
Total Burn Steps	3
Fuel Volume [cc]	362.4
Assembly Power [MWt]	1.11
Internal Burn Steps	50
Predictor Steps	1

2.2. MCNP kcode Parameter Determination

To determine the MCNP kcode parameters, the actual tallies that MONTEBURNS creates were run separately in MCNP. There are two types of tallies present, both of which are of the volumetric type F4, used to calculate a six group neutron flux and reaction rates [4]. While these are automatically created by MONTEBURNS, the MCNP kcode parameters must be carefully chosen to provide accurate solutions with appropriate uncertainties while optimizing CPU time. The minimum kcode parameters should at a minimum provide enough particle histories for both of the F4 tallies to pass their default 10 statistical checks. The balance of these particles between number of kcode steps and the number of particles per step is also important to achieve accurate k-effective results.

This model was run 200 times, so optimizing CPU time was a critical factor in determining the kcode parameters. The minimum number of particle histories while passing the statistical checks was chosen. Generally for accurate k-effective results, the number of kcode steps is chosen to be large while at the same time for minimal flux tally uncertainty the number of particles per step is chosen to be large and an optimal parameter set must be selected. The kcode parameters chosen for this study are shown in Table II.

Table II. MCNP kcode Parameters.

Parameter	Value
Particles Per Step	3000
Initial k-effective Guess	1
Steps to Skip	25
Total Number of Steps	100

2.3. Results

The model from Figure1 was run 200 times using MONTEBURNS. The results are broken into three categories: fission products, uranium isotopes, and k-effective. Due to the random nature of the Monte-Carlo process, this procedure was expected to produce results that formed a normal distribution.

2.3.1. Fission product results

Eight fission products (Table III) were tracked using MONTEBURNS. These include a strong absorber (^{135}Xe) and short, medium, and long lived isotopes. Although this model did not include any decay step post irradiation, these isotopes provide an appropriate statistical benchmark.

Table III. Fission Products Tracked.

Element	Half Life	Fission Yield [%]
Kr-85	3934.4 d	0.2180
Sr-90	28.79 y	4.505
Tc-99	211,000 y	6.1385
I-131	8.02 d	2.8336
I-135	6.57 h	6.33
Xe-135	9.1 h	6.33 [effective]
Cs-125	2,300,000 y	6.9110
Cs-137	30.07 y	6.337

Figure 2 shows a frequency distribution for ^{131}I at the end of each burnup step with the center bin over the mean. ^{131}I is a short lived weak absorber. The isotopic mass was normalized to the average at each burnup step for comparison. The average ^{131}I mass at the end of each step was

0.1870g ± 0.20%, 0.2799g ± 0.158%, and 0.3242g ± 0.145% for steps one, two, and three, respectively. So if the results were normally distributed, then the peak would be centered at unity and the data points would be symmetric about unity, for each burnup step.

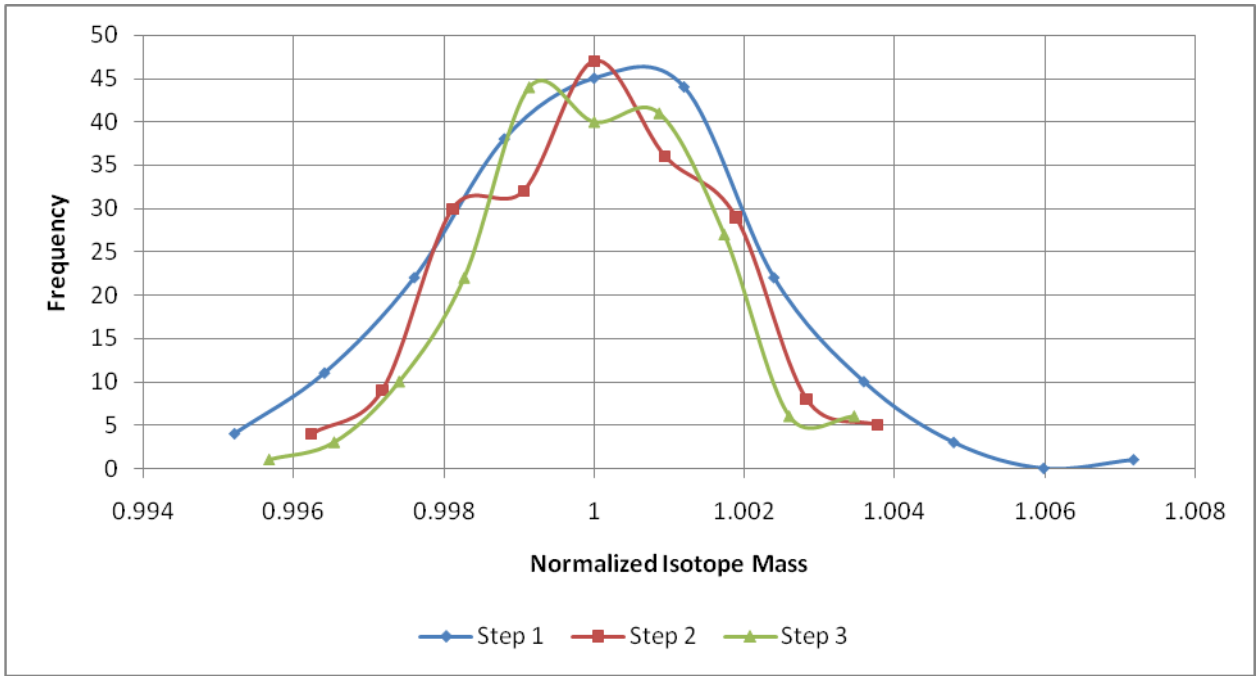

Figure 2. ^{131}I distribution at each burnup step.

In the first step, the peak is located on the center bin. The bins directly to either side of the peak are not symmetric, but the outer bins are. The non-symmetric point to the right of the peak and the tail on the high side suggest may be attributed to a few outlier points since the other bins are relatively symmetric. Step two shows similar results with symmetric bins with the exception of the bins on either side of the peak. The third step shows a unique result likely due to a round off error described in 2.3.2.

The next isotope examined was ^{135}Xe. ^{135}Xe has a short half-life of 9.1h and a strong absorption cross section of $2x10^6$b. During a constant irradiation, it establishes an equilibrium concentration in about 1-2 days. This was modeled several times using MONTEBURNS and the same infinite lattice assembly with different total burn lengths and burnup steps to access the impact of equilibrium conditions on the statistical analysis (which used a burnup step length of 8.5d). Figure 3 shows results for a 2.5d burn, 2d shutdown, and an additional 1.5d burn. This shows the maximum flux perturbation of just over 5%.

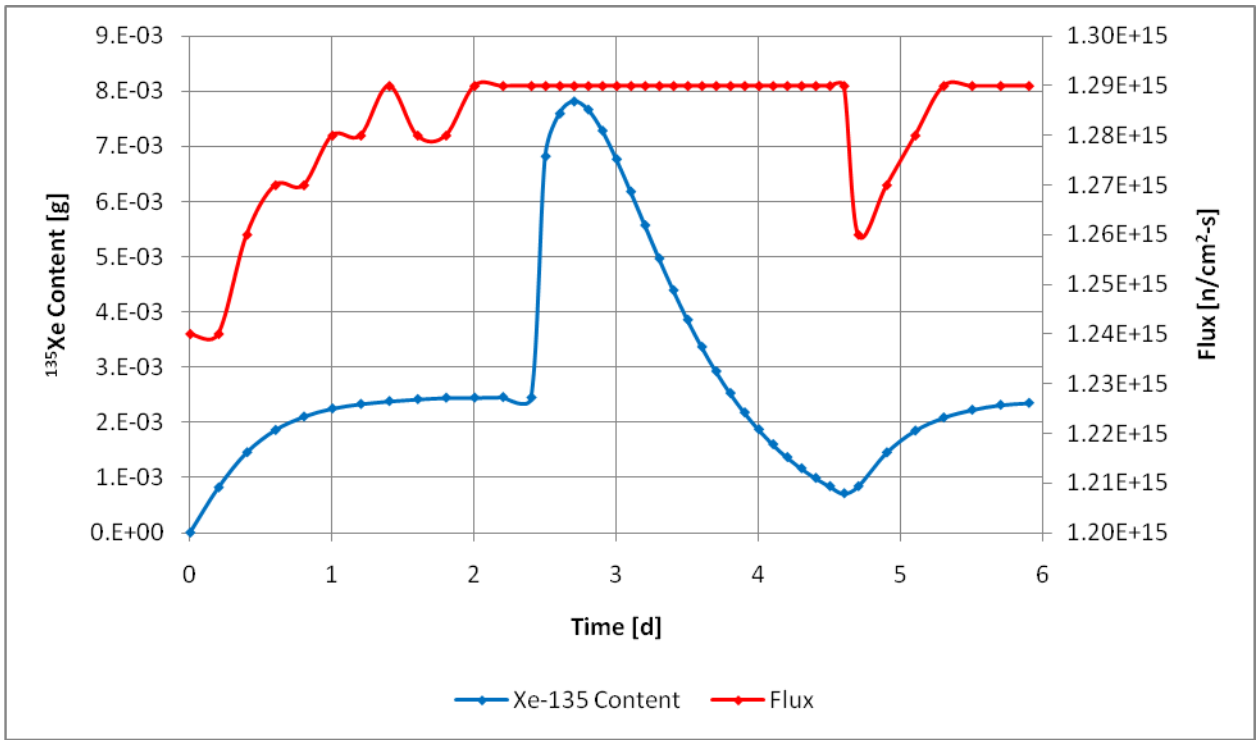

Figure 3. ^{135}Xe saturation calculation results.

MONTEBURNS only reports three significant digits on its flux output. Round off and statistical uncertainty produces the oscillations in the flux results. During decay steps, MONTEBURNS reports the flux from the last burn step instead of properly reporting zero shown above. The modeled burnup step length for the statistical analysis is 8.5d, so no effects of reaching equilibrium xenon levels are present with a saturation time of approximately 1-2d. With a strong decay and interaction removal rate, it may be expected to see a non-symmetric distribution on either side of the distribution mean.

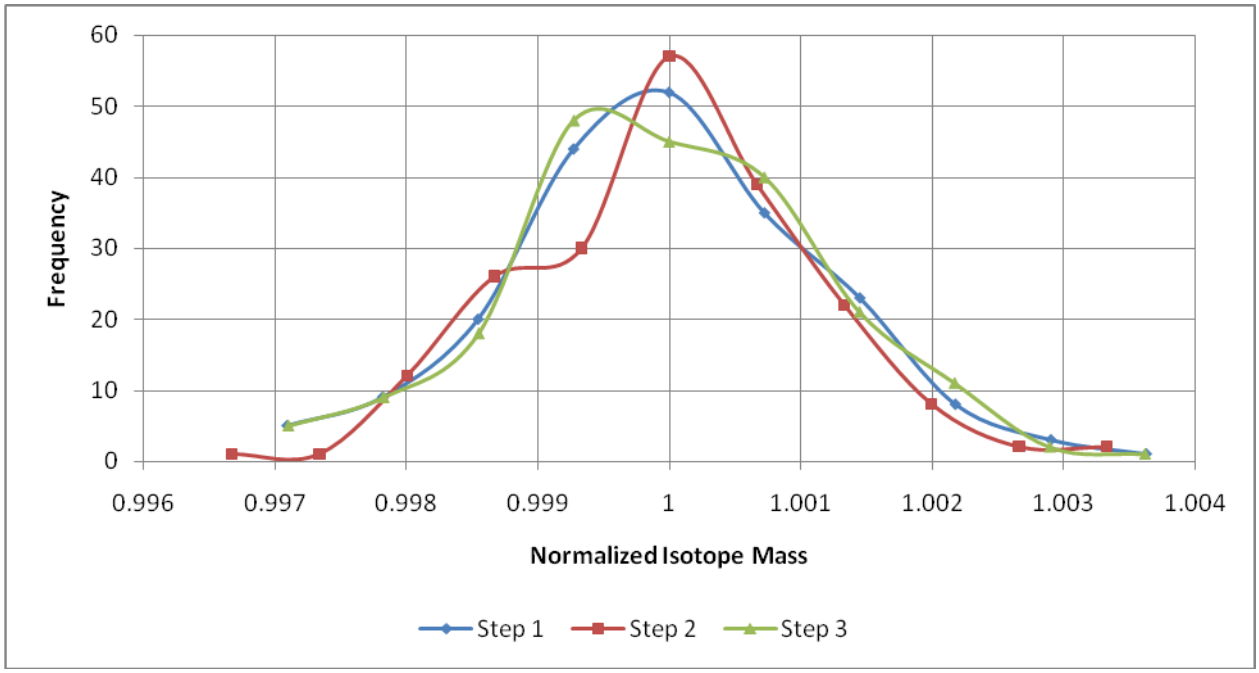

Figure 4. ^{135}Xe distribution at each burnup step.

The first two burnup steps for ^{135}Xe (Figure 4) possess a mean on left side of the peak while the third step distribution center shifts back toward the mean. The ^{135}Xe average mass at the end of each step was 0.00236g ± 0.122%, 0.00225g ± 0.111%, and 0.00259g ± 0.121% for steps one, two, and three, respectively. Detailed histograms from all recorded fission products are shown in Appendix C.

All three resulting distributions were steeper on the lower side of the peak than the higher and the first and third steps trailed further on the higher side also. The peak on the third step was not located on the center bin which may be a result from the round off error and uncertainty propagated.

2.3.2. Uranium results

The reactor initial uranium isotopics consisted of ^{234}U, ^{235}U, ^{236}U, and ^{238}U in the quantities shown in Table IV. The uranium was in the form of U_3O_8 mixed with aluminum.

Table IV. Initial Uranium Isotopics.

Isotope	Mass Percent [%]	Initial Mass [g]
^{234}U	0.2489	3.064
^{235}U	23.16	285.1
^{236}U	0.1076	1.325
^{238}U	1.347	16.58

MONTEBURNS uses text files to pass information between MCNP and ORIGEN. In MONTEBURNS, the default level of accuracy is set to return only three digits [1]. This was modified to return nine digits from the mass calculations; however, only five of these digits are meaningful since that is the number of significant digits passed from the MCNP tallies. These five digit reaction rate and flux tallies are passed to the reactor power and fuel volume normalizations and used in the mass calculations which report nine digits. In the fission product calculations, the statistically varying digit was well before the fifth digit that is rounded. Due to the high concentrations of uranium and the size of the fuel volume, the statistically varying digit for the uranium isotopes falls in the same place as the round off digit. This process creates a distribution of binned rounded values which cannot be avoided without modifying the MCNP source code or using multiple lower volume cells.

To easily visualize the round off error, a histogram of the uranium isotopes using 100 bins was created which can be seen in Appendix D. To show the data consistently, the histograms in Figure 5 were created using the same number of bins as the number of points rounded to or less. Similar to the fission products, the ^{235}U distributions are centered to the right of the mean mass. The mean masses and standard deviations for each step were 272.77g ± 0.010%, 260.50g ± 0.014%, and 248.26g ± 0.020%.

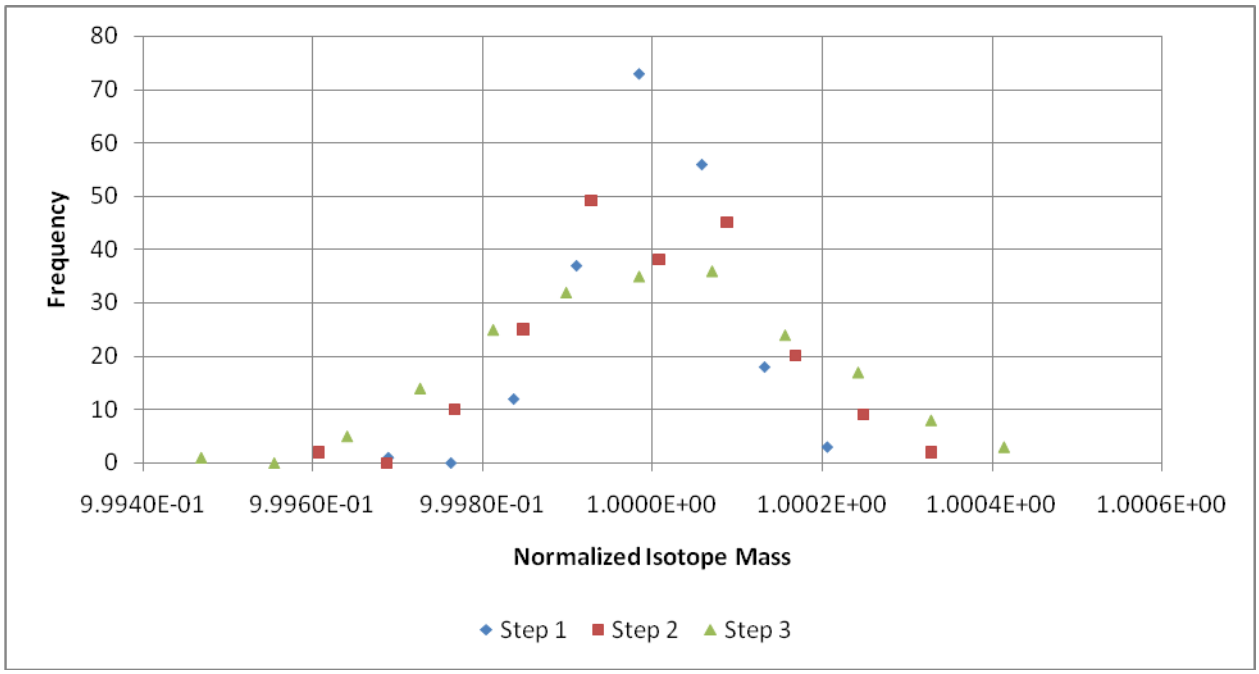

Figure 5. ^{235}U distribution at the end of burnup step 1.

The ^{235}U distributions are actually sets of discrete points due to the round off error. After the first burnup step, the eight discrete points still form a normal distribution. After the second step, the statistical variance increases and after the round off is spread over ten discrete points. This distribution is very non-Gaussian with the round off forming two peaks of lower frequency. This trend continues for the third step where the distribution widens more with an even lowered peak and the distribution spreads to twelve discrete points.

2.3.3. k-effective results

The frequency distribution for k-effective is shown in Figure 6. The k-effective results from the initial step, or zeroth step, are a direct function of the random number seeds. In the initial step, the k-effective should form a true normal distribution. In further steps, as uncertainties exist and isotopic distributions had slightly shifted due to the round off, it is expected to see a shift in k-effective.

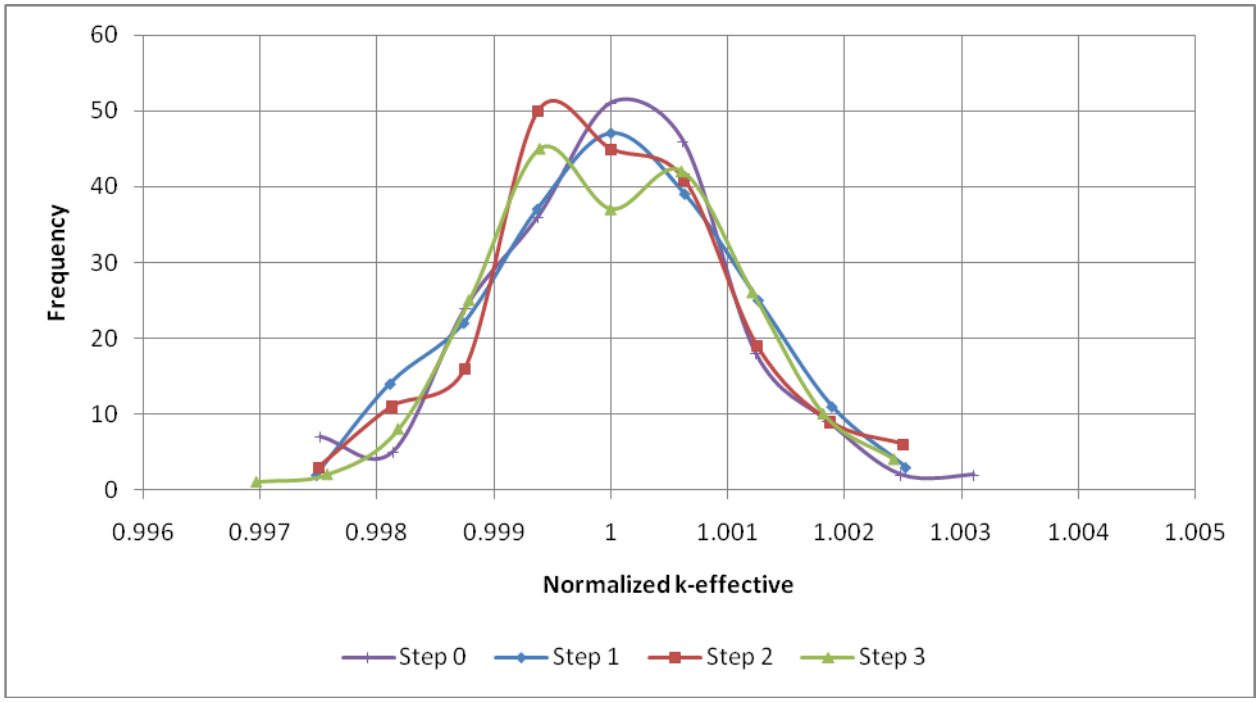

Figure 6. MCNP k-effective distribution at each burnup step.

The mean k-effective and standard deviation for each step were 1.522 ± 0.104%, 1.450 ± 0.1056%, 1.426 ± 0.1048%, and 1.413 ± 0.1015%. Since every step uses the same quantity of histories, it was expected that the uncertainty in each step's k-effective would be similar. In first step, as there becomes variation in the ^{235}U quantity, the k-effective distribution flattens and spreads outward. This effect was expected as a direct propagation of uncertainty. In the second and final steps, side effects from the round off propagated throughout creating a unique distribution. Detailed histograms from the k-effective results may be seen in Appendix E.

All of the isotope results are summarized in Table V. Many of the fission products have similar uncertainties for each step. This makes sense due to the number of fissions being consistent with a constant power specified.

Table V. Summary of mass and k-effective results.

Isotope	Step 1 [g]	Step 2 [g]	Step 3 [g]
Kr-85	$9.48 \times 10^{-3} \pm 0.202\%$	$1.93 \times 10^{-2} \pm 0.153\%$	$2.90 \times 10^{-2} \pm 0.128\%$
Sr-90	$0.206 \pm 0.201\%$	$0.411 \pm 0.157\%$	$0.616 \pm 0.126\%$
Tc-99	$0.131 \pm 0.203\%$	$0.353 \pm 0.156\%$	$0.582 \pm 0.130\%$
I-131	$0.187 \pm 0.200\%$	$0.280 \pm 0.158\%$	$0.324 \pm 0.145\%$
I-135	$1.53 \times 10^{-2} \pm 0.198\%$	$1.53 \times 10^{-2} \pm 0.198\%$	$1.53 \times 10^{-2} \pm 0.209\%$
Xe-135	$2.36 \times 10^{-3} \pm 0.122\%$	$2.25 \times 10^{-3} \pm 0.111\%$	$2.13 \times 10^{-3} \pm 0.121\%$
Cs-125	$3.65 \times 10^{-2} \pm 0.114\%$	$7.30 \times 10^{-2} \pm 0.075\%$	$1.08 \times 10^{-1} \pm 0.062\%$
Cs-137	$0.345 \pm 0.202\%$	$0.690 \pm 0.153\%$	$1.03 \pm 0.129\%$
U-234	$3.00 \pm 0.024\%$	$2.94 \pm 0.033\%$	$2.88 \pm 0.041\%$
U-235	$2.73 \times 10^{2} \pm 0.010\%$	$2.60 \times 10^{2} \pm 0.014\%$	$2.48 \times 10^{2} \pm 0.020\%$
U-236	$3.76 \pm 0.130\%$	$6.15 \pm 0.110\%$	$8.51 \pm 0.102\%$
U-238	$16.5 \pm 0.008\%$	$16.4 \pm 0.013\%$	$16.2 \pm 0.015\%$

2.3.4. Statistical test results.

To test if the distributions were normal they were tested against a normal distribution using the χ^2 test at α of 0.05 and 0.10. These tests were performed using eight bins with five degrees of freedom since two parameters are estimated. The null hypothesis in these tests is that the distribution is not normal. The results of these tests for k-effective are shown in Table V. The test statistic was compared to 11.07 and 9.24. In the test of α equals 0.05, the first three steps failed to reject the null hypothesis. In the final step the null hypothesis was rejected being statistically not normally distributed.

Table VI. χ^2 distribution tests for k-effective.

Step	χ^2 Statistic	Reject Null (α=0.05, χ^2<11.07)	Reject Null (α=0.10, χ^2<9.24)
0	3.303	No	No
1	2.525	No	No
2	10.28	No	Yes
3	11.37	Yes	Yes

In the case of α equals 0.10, the final two steps rejected the null hypothesis. In the k-effective tests the χ^2 statistic is growing as the uncertainty propagates through the steps. These results suggest greater kcode parameters may be required to stabilize error propagation. The same test was done on the mass distributions for ^{135}Xe and the results are shown in Table V.

Table VII. χ^2 distribution tests for ^{135}Xe.

Step	χ^2 Statistic	Reject Null (α=0.05, χ^2<11.07)	Reject Null (α=0.10, χ^2<9.24)
1	2.894	No	No
2	8.167	No	No
3	4.802	No	No

In the ^{135}Xe tests, the χ^2 statistic begins quite small then grows close to the rejection point and then is reduced back down again. While some of the histograms do not suggest these distributions to be normal, the null hypothesis that the distribution is not normal is rejected in each step. The high statistic in the second step may be partially attributed due to the round off from the uranium isotopes. This same test was performed on ^{131}I, in which all six tests failed to reject the null hypothesis as well.

3. CONCLUSIONS

The Monte-Carlo depletion routine MONTEBURNS possesses an uncertainty in its reaction rate and flux tallies. This information is not passed on or propagated though the burnup steps. A statistical analysis to examine and understand this uncertainty as well as its effect on variation in isotope generation and depletion was performed. A simple infinite lattice assembly level model of the ORR was burned using 3 burnup steps in 200 separate runs using different random number seeds. These results created a distribution of k-effective and fission products.

To examine a greater accuracy solution, the results were created using nine significant digits as opposed to the default three. Of these nine digits only five of them are of value because the flux solution has only five digits. The majority of the results for fission products show statistically normal distributions after the first burnup step, but a rounding error occurs in the high quantity uranium isotopes where the statistically varying digit is the fifth. Instead of a true random distribution of results, the round off creates a set of discrete values.

It can be concluded that if a high accuracy solution is desired with many burnup steps, it is best to keep the material mass less than 100g to minimize the round off effects and provide statistically random results. The distribution of k-effective results initially shows a normal distribution and then properly widens as system uncertainty propagates. The final k-effective steps show unique results from side effects of the round off error. Statistic analysis of these distributions was performed against a normal distribution using the χ^2 test. The fission product tests fail to reject the null hypothesis, while the χ^2 test statistic grows significantly in the k-effective test. This suggests that although some of the isotopes appear to have a bias, statistically

they are still normally distributed. While some of the uncertainty propagation may be attributed to the uranium round off error, the k-effective tests suggest greater kcode parameters should be used.

ACKNOWLEDGMENTS

I would like to acknowledge Donna L. Beals and Roger Webb of Savannah River National Laboratory's Nonproliferation Technology Section for funding, support, and data.

REFERENCES

1. D. I. Poston and H. R. Trellue, "Users Manual, Version 1.0 for MONTEBURNS, Version 3.01," Los Alamos National Laboratory, 1998.
2. Laboratory O.R.N, "ORIGEN 2.2: Isotope generation and depletion code matrix exponential method," Department of Energy, RSICC, Oak Ridge, (2002).
3. Oak Ridge National Laboratory, "Oak Ridge Research Reactor: Appendix A, 19 Plate, U_3O_8, HEU, Rev., 7" United States Department of Energy, (1997).
4. Monte Carlo X Team, "MCNP—A general Monte Carlo N-particle transport code, Version 5," Department of Energy, Los Alamos National Laboratory, Los Alamos, (2005).

APPENDIX A

MCNP model of ORR in an infinite lattice configuration

```
ORR Fuel Assembly
c Matthew Sternat 8/11/2010
c
c
c sideplates-------------------------------------------------------------------
1    5 -2.7268  ((-24  23):(19 -20)) 3 -4 -18 31                          imp:n=1
3    5 -2.7268  ((-24  23):(19 -20)) 3 -4 -32 17                          imp:n=1
c water
5    1 -1 33 -34 31 -32 3 -4 (219:24:-19) (-101:24:-19) #1  #3            imp:n=1
c cladding for plates----------------------------------------------------------
11   5 -2.7268 20 -23 3 -4 ((101 -201):(119 -219)) #31                    imp:n=1
12   5 -2.9546 20 -23 11 -12 ((102 -202) : (103 -203) : (104 -204) : &
     (105 -205) : (106 -206) : (107 -207) : (108 -208) : (109 -209) : &
     (110 -210) : (111 -211) : (112 -212) : (113 -213) : (114 -214) : &
     (115 -215) : (116 -216) : (117 -217) : (118 -218) : (120 -220) : &
     (141)) 31 -32 #32                                                    imp:n=1
c fuel meat--------------------------------------------------------------------
31   3 -3.396 5 -6  7  -8  ((121 -221):(139 -239))                        imp:n=1
32   3 -3.396 13 -14 15 -16 ((122 -222) : (123 -223) : (124 -224) : &
     (125 -225) : (126 -226) : (127 -227) : (128 -228) : (129 -229) : &
     (130 -230) : (131 -231) : (132 -232) : (133 -233) : (134 -234) : &
     (135 -235) : (136 -236):(137 -237):(138 -238):(140 -240)) 31 -32    imp:n=1
c coolant channels-------------------------------------------------------------
51   1 -1 20 -23 ((-102 201) : (-103 202) : (-104 203) : (-105 204) : &
     (-106 205) : (-107 206) : (-108 207) : (-109 208) : (-110 209) : &
     (-111 210) : (-112 211) : (-113 212) : (-114 213) : (-115 214) : &
     (-116 215) : (-117 216) : (-118 217) : (-119 218) : (-141 210) : &
     (220 -111)) 31 -32 3 -4                                              imp:n=1
c    water above/below
72   1 -1 20 -23  12 -4 ((102 -202) : (103 -203) : (104 -204) : (105 -205) : &
     (106 -206) : (107 -207) : (108 -208) : (109 -209) : (110 -210 -32) : &
     (111 -211 31) : (112 -212) : (113 -213) : (114 -214) : (115 -215) : &
     (116 -216) : (117 -217) : (118 -218):-220:141) 31 -32                imp:n=1
91   1 -1 20 -23 -11  3 ((102 -202) : (103 -203) : (104 -204) : (105 -205) : &
     (106 -206) : (107 -207) : (108 -208) : (109 -209) : (110 -210 -32) : &
     (111 -211 31) : (112 -212) : (113 -213) : (114 -214) : (115 -215) : &
     (116 -216) : (117 -217) : (118 -218):-220:141) 31 -32                imp:n=1
c void and upper/lower water
901  1 -1 -3  35 31 -32 33 -34                                            imp:n=1
902  1 -1  4 -36 31 -32 33 -34                                            imp:n=1
999  0 (-35:36:-31:32:-33:34)                                             imp:n=0

c surface descriptions
c plate dimensions (outer)
3    pz -34.4488
4    pz  34.4488
c fuel meat (outer)
5    px  -3.138805
6    px   3.138805
7    pz -29.90215
8    pz  29.90215
c surface descriptions
c plate dimensions (inner)
11   pz -31.2738
12   pz  31.2738
c fuel meat (inner)
13   px  -3.140075
14   px   3.140075
```

```
15   pz -29.89199
16   pz  29.89199
c side plates (left)
17   py  3.7575
18   py  3.70593
19   px -3.65857
20   px -3.49477
c (Right)
23   px 3.49477
24   px 3.65857
c outer shell
32   -32 py 8.100001
31   -31 py 0.000001
33   -34 px -3.7
34   -33 px 3.7
35   pz -150
36   pz  150
c curvature for plates and spacing (note starts from bottom)
c centered at 0
c 100 series "lower" side 200 series "upper" side of plate
101  c/z 0.0 -09.7054 13.97
102  c/z 0.0 -09.2431 13.97
103  c/z 0.0 -08.8215 13.97
104  c/z 0.0 -08.3998 13.97
105  c/z 0.0 -07.9782 13.97
106  c/z 0.0 -07.5566 13.97
107  c/z 0.0 -07.1349 13.97
108  c/z 0.0 -06.7133 13.97
109  c/z 0.0 -06.2916 13.97
110  c/z 0.0 -05.8700 13.97
111  c/z 0.0 -13.5484 13.97
112  c/z 0.0 -13.1267 13.97
113  c/z 0.0 -12.7051 13.97
114  c/z 0.0 -12.2834 13.97
115  c/z 0.0 -11.8618 13.97
116  c/z 0.0 -11.4402 13.97
117  c/z 0.0 -11.0185 13.97
118  c/z 0.0 -10.5969 13.97
119  c/z 0.0 -10.1752 13.97
c
c added two
120  c/z 0.0 -13.9700 13.97
141  c/z 0.0 -5.44840 13.97
c upper
201  c/z 0.0 -09.5416 13.97
202  c/z 0.0 -09.1156 13.97
203  c/z 0.0 -08.6940 13.97
204  c/z 0.0 -08.2723 13.97
205  c/z 0.0 -07.8507 13.97
206  c/z 0.0 -07.4291 13.97
207  c/z 0.0 -07.0074 13.97
208  c/z 0.0 -06.5858 13.97
209  c/z 0.0 -06.1641 13.97
210  c/z 0.0 -05.7425 13.97
211  c/z 0.0 -13.4209 13.97
212  c/z 0.0 -12.9992 13.97
213  c/z 0.0 -12.5776 13.97
214  c/z 0.0 -12.1559 13.97
215  c/z 0.0 -11.7343 13.97
216  c/z 0.0 -11.3127 13.97
217  c/z 0.0 -10.8910 13.97
218  c/z 0.0 -10.4694 13.97
219  c/z 0.0 -10.0114 13.97
```

```
c
c added one
220  c/z 0.0 -13.8425 13.97
c fuel meat 121-139 lower
121  c/z 0.0 -09.64890 13.97
122  c/z 0.0 -09.20477 13.97
123  c/z 0.0 -08.78313 13.97
124  c/z 0.0 -08.36149 13.97
125  c/z 0.0 -07.93985 13.97
126  c/z 0.0 -07.51821 13.97
127  c/z 0.0 -07.09657 13.97
128  c/z 0.0 -06.67493 13.97
129  c/z 0.0 -06.25329 13.97
130  c/z 0.0 -05.83165 13.97
131  c/z 0.0 -13.51001 13.97
132  c/z 0.0 -13.08837 13.97
133  c/z 0.0 -12.66673 13.97
134  c/z 0.0 -12.24509 13.97
135  c/z 0.0 -11.82345 13.97
136  c/z 0.0 -11.40181 13.97
137  c/z 0.0 -10.98017 13.97
138  c/z 0.0 -10.55853 13.97
139  c/z 0.0 -10.11870 13.97
c
c added one
140  c/z 0.0 -13.93165 13.97
c  fuel meat 221-239 upper
221  c/z 0.0 -09.598100 13.97
222  c/z 0.0 -09.153962 13.97
223  c/z 0.0 -08.732322 13.97
224  c/z 0.0 -08.310682 13.97
225  c/z 0.0 -07.889042 13.97
226  c/z 0.0 -07.467402 13.97
227  c/z 0.0 -07.045762 13.97
228  c/z 0.0 -06.624122 13.97
229  c/z 0.0 -06.202482 13.97
230  c/z 0.0 -05.780842 13.97
231  c/z 0.0 -13.459202 13.97
232  c/z 0.0 -13.037562 13.97
233  c/z 0.0 -12.615922 13.97
234  c/z 0.0 -12.194282 13.97
235  c/z 0.0 -11.772642 13.97
236  c/z 0.0 -11.351002 13.97
237  c/z 0.0 -10.929362 13.97
238  c/z 0.0 -10.507722 13.97
239  c/z 0.0 -10.067900 13.97
c
c added one
240  c/z 0.0 -13.880842 13.97

c materials
m1   1001 .333
     8016 .667
     nlib=70c
mt1  lwtr.64t
c fuel meat-------------------------------------------------------------------
m3   92234 -0.002489399
     92235 -0.231647947
     92236 -0.00107687
     92238 -0.013474275
     8016  -0.045094134
     13027 -0.706217375
     nlib=70c
```

```
c m4   92235 -0.231552976
c      92238 -0.017061798
c       8016 -0.045191829
c      13027 -0.706193397
c      nlib=70c
c aluminum-----------------------------------------------------------------------
m5   13027 1
     nlib=70c
c source-------------------------------------------------------------------------
mode n
kcode 3000 1 25 100
ksrc 0 3.87 0  0 3.87 25  0 3.87 -25  -2.4 6.69 0  -2.4 6.69 -25  -2.4 6.69 25
     2.4 6.69 0  2.4 6.69 -25  2.4 6.69 25  -2.4 1.12 0  -2.4 1.12 -25
     -2.4 1.12 25  2.4 1.12 0  2.4 1.12 -25 2.4 1.12 25
c sdef cel d1 axs  0 0 1  rad d5 ext d6 pos 0 4 -35 eff 0.0001
c si1  L 31 32
c sp1  0.105263157894736842105263157894 74 0.894736842105263157894736842105 26
c si5  0 6
c si6  0 70
rand seed=1
```

APPENDIX B

MONTEBURNS input deck.

```
ORR inf lattice
PC         ! Type of operating system
1          ! Number of MCNP materials to burn
3          ! MCNP material number #1 (must be less than 100)
362.38662  ! Material #1 volume (cc), input 0 to use mcnp value (if exists)
1.11       ! Power in MWt (for the entire system modeled in mcnp deck)
-200.      ! Recov. energy/fis (MeV); if negative use for U235, ratio other isos
25.5       ! Total number of days burned (used if no feed)
3          ! Number of outer burn steps
50         ! Number of internal burn steps (multiple of 10)
1          ! Number of predictor steps (+1 on first step), 1 usually sufficient
0          ! Step number to restart after (0=beginning)
FFTFC      ! number of default origen2 lib - next line is origen2 lib location
c:/mb/origen22/libs
.00001     ! fractional importance (track isos with abs,fis,atom,mass fraction)
0          ! Intermediate keff calc. 0) No 1) Yes
14         ! Number of automatic tally isotopes, followed by list.
8016.70c
13027.70c
36085.70c
38090.70c
43099.70c
53131.70c
53135.70c
54135.70c
55135.70c
55137.70c
92234.70c
92235.70c
92236.70c
92238.70c
```

APPENDIX C

Detailed fission product results figures.

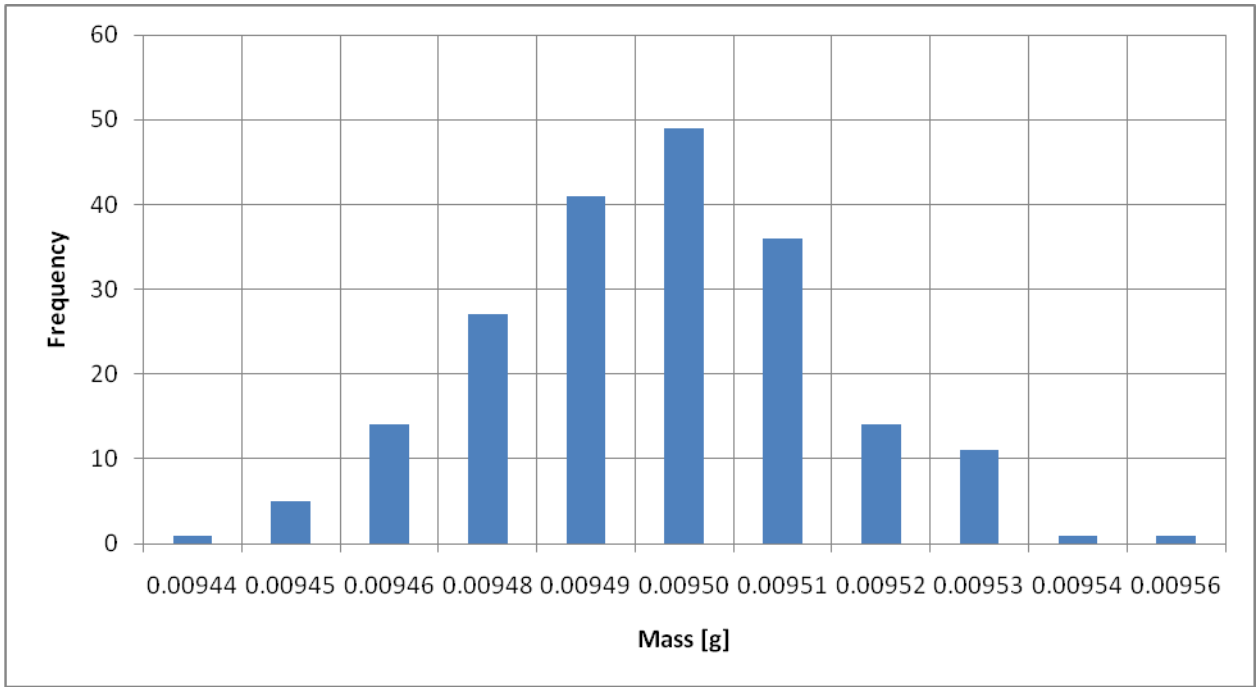

Figure 7. ^{85}Kr step 1 mass distribution.

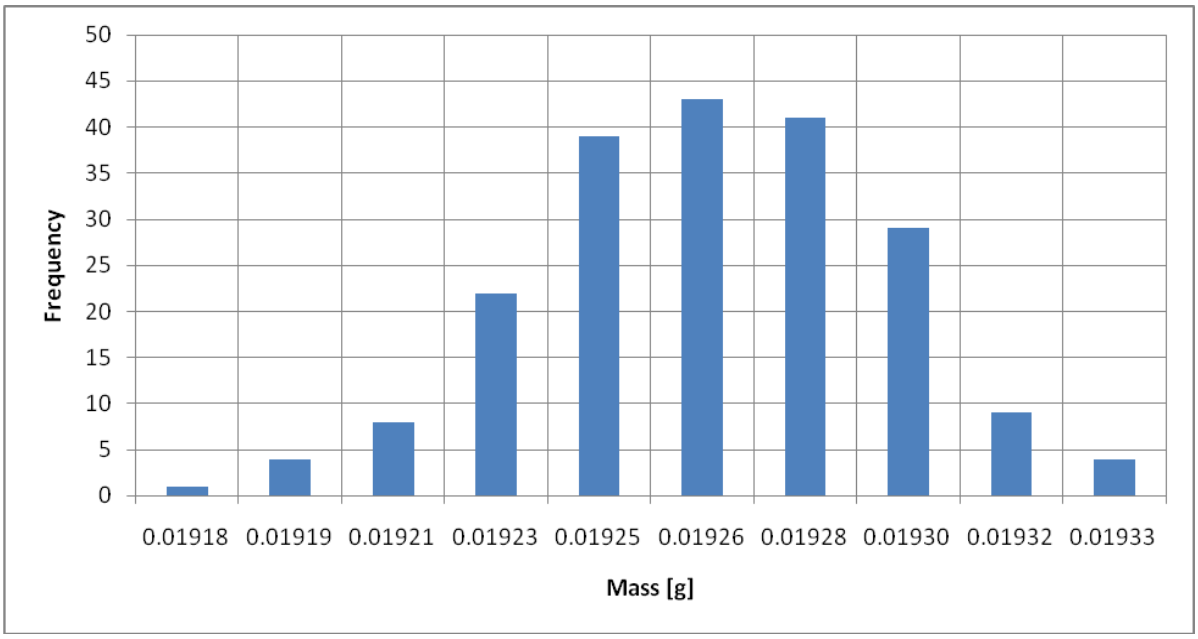

Figure 8. ^{85}Kr step 2 mass distribution.

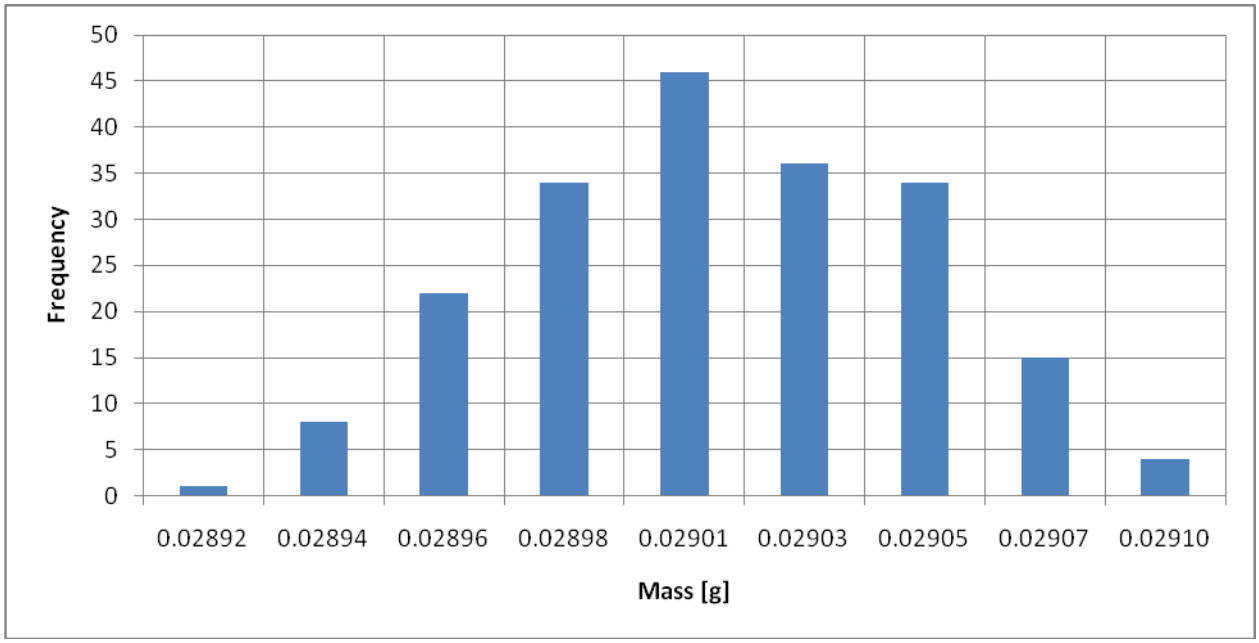

Figure 9. ^{85}Kr step 3 mass distribution.

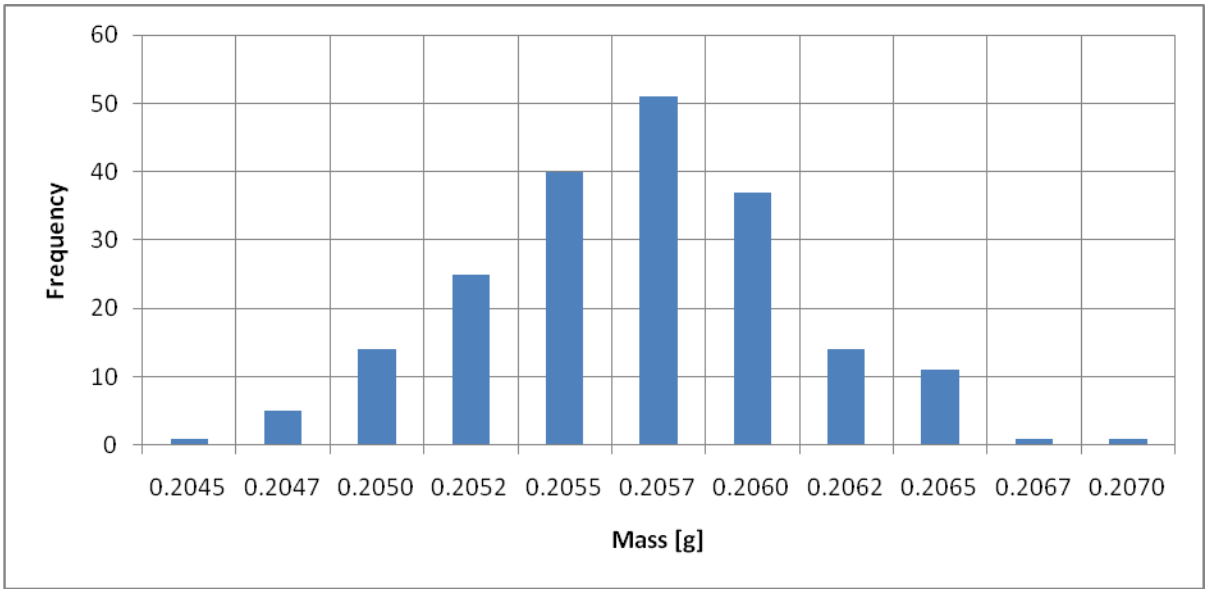

Figure 10. ^{90}Sr step 1 mass distribution.

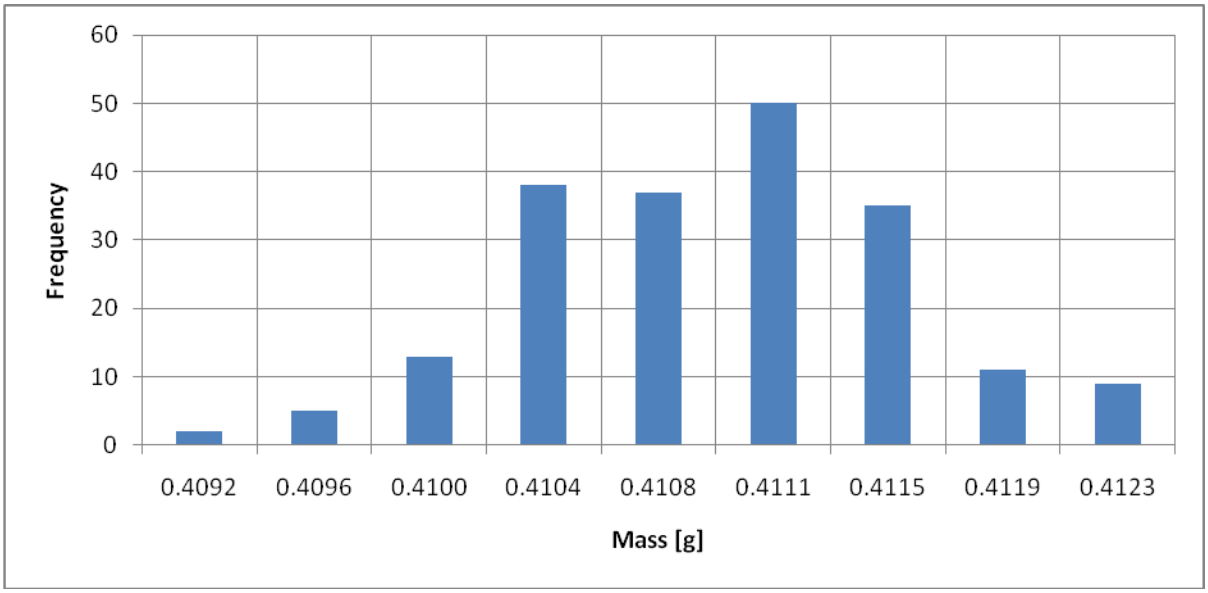

Figure 11. ^{90}Sr step 2 mass distribution.

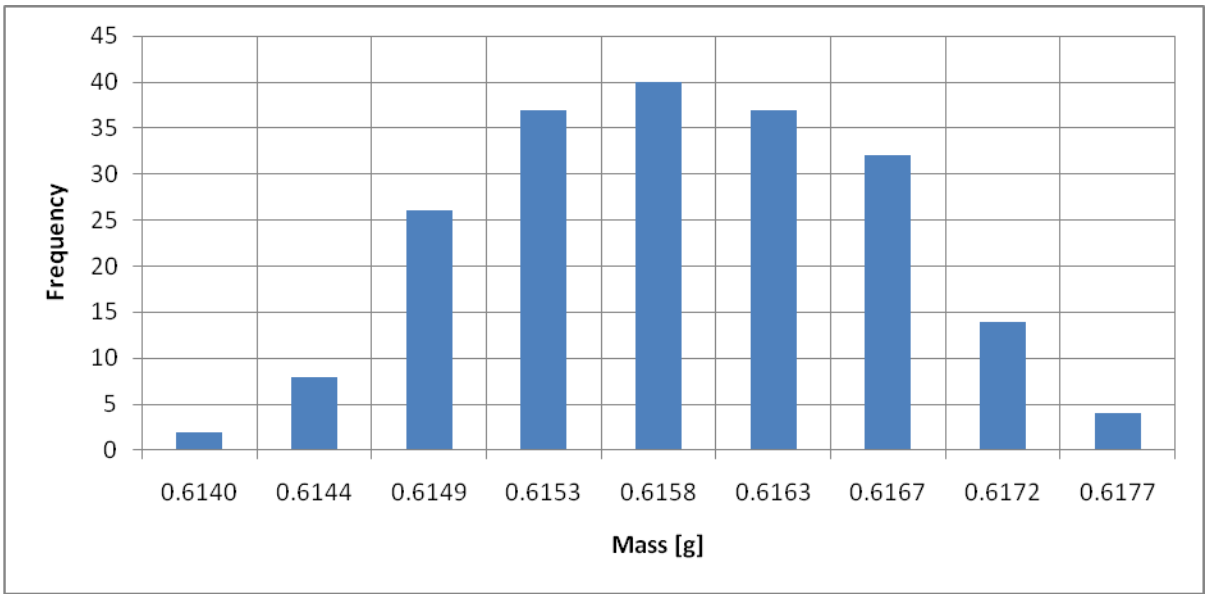

Figure 12. ^{90}Sr step 3 mass distribution.

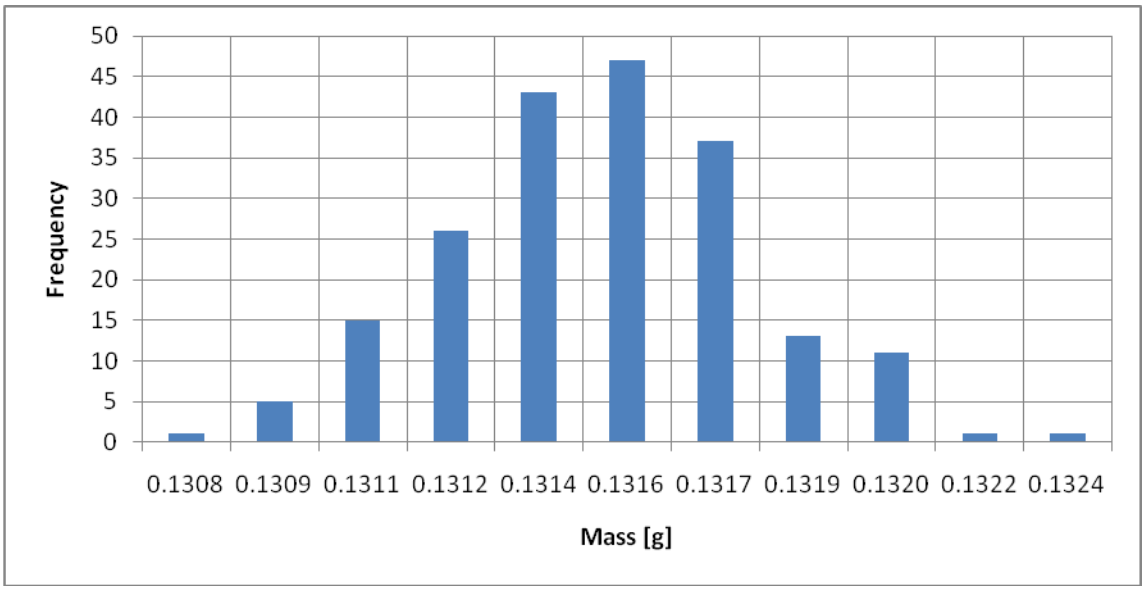

Figure 13. ^{99}Tc step 1 mass distribution.

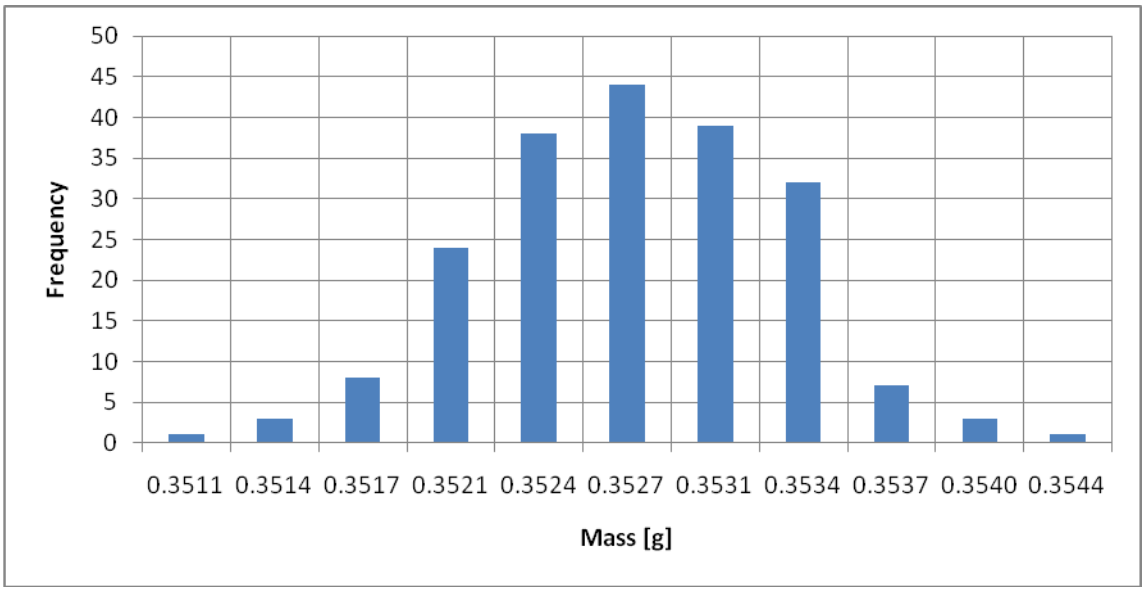

Figure 14. ^{99}Tc step 2 mass distribution.

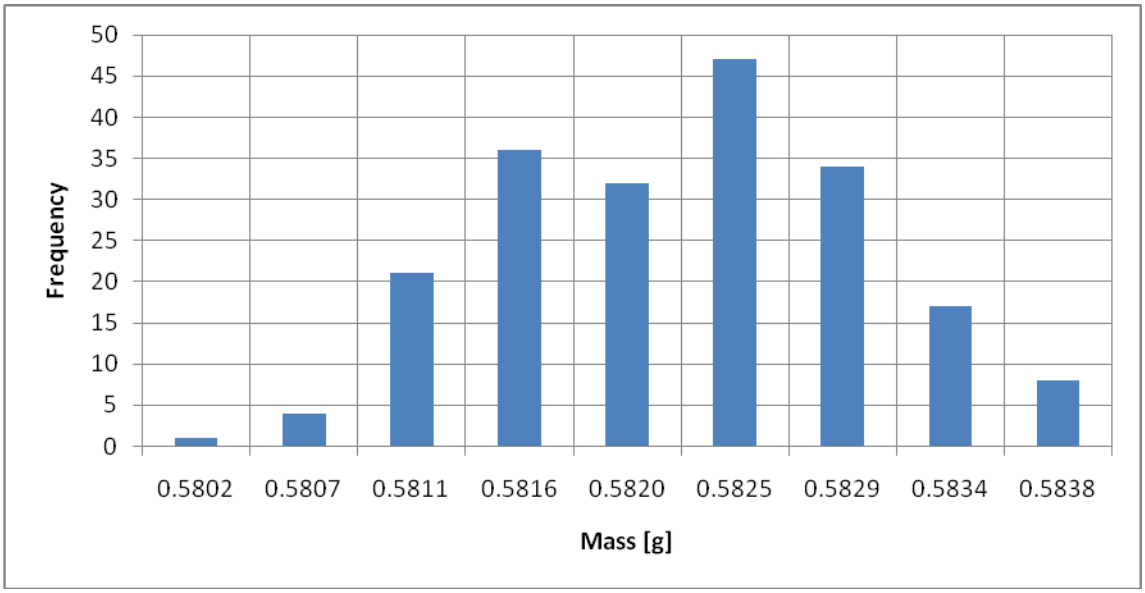

Figure 15. ^{99}Tc step 3 mass distribution.

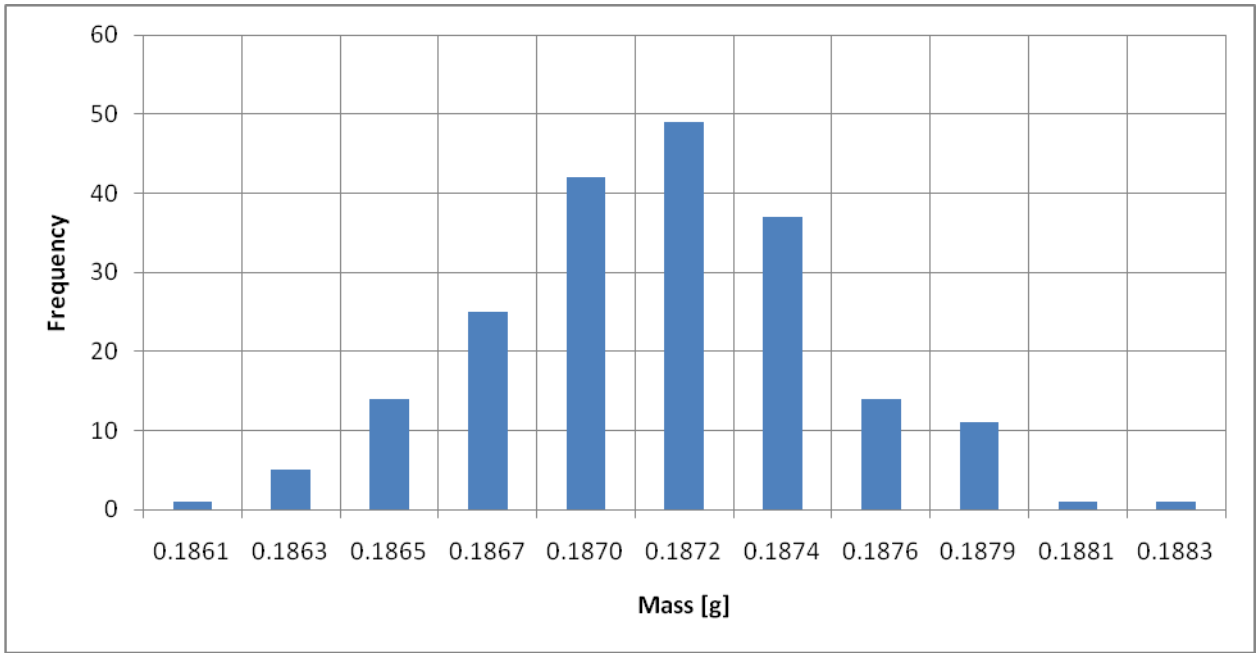

Figure 16. ^{131}I step 1 mass distribution.

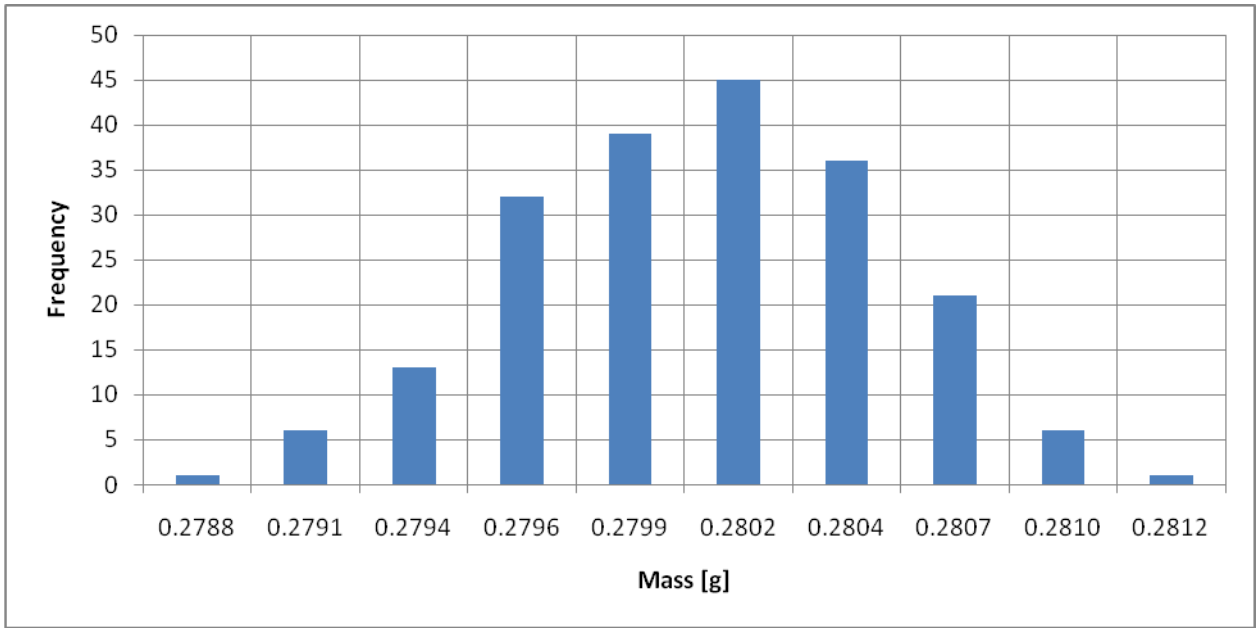

Figure 17. ^{131}I step 2 mass distribution.

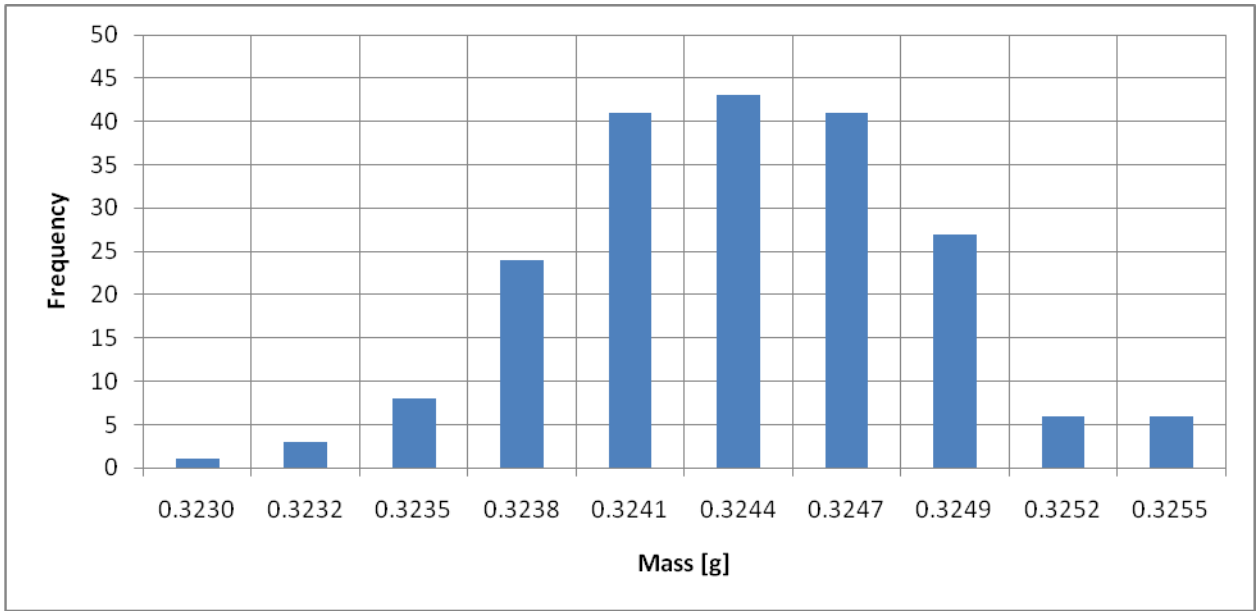

Figure 18. ^{131}I step 3 mass distribution.

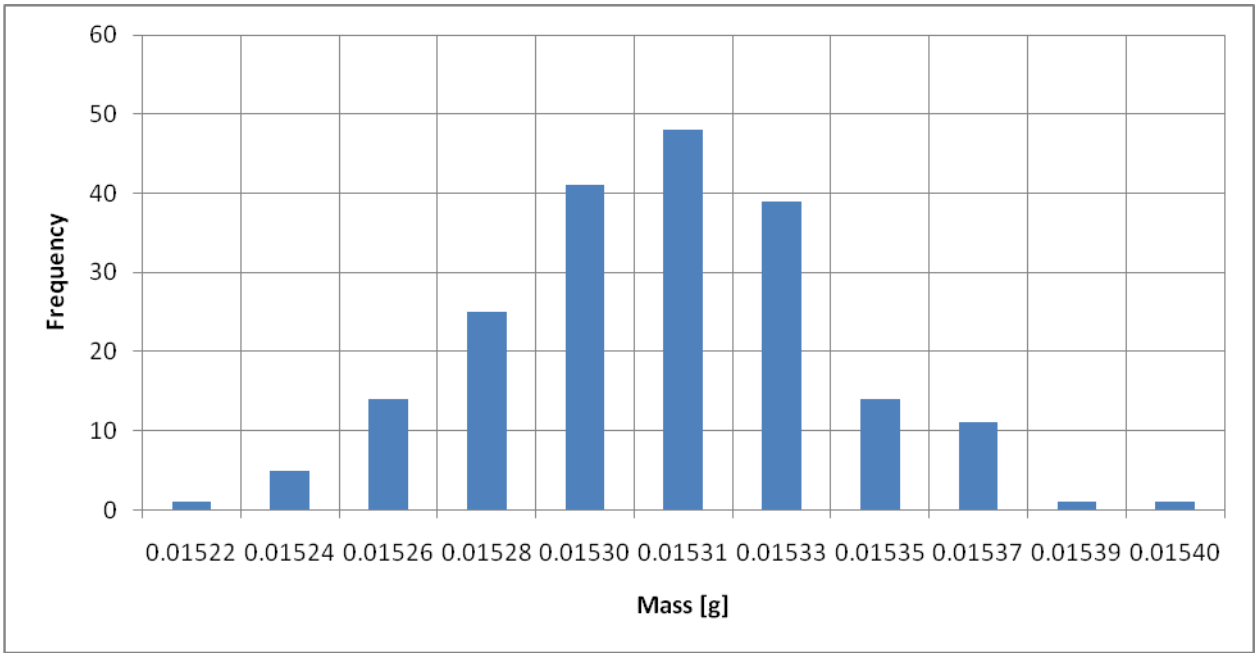

Figure 19. ^{135}I step 1 mass distribution.

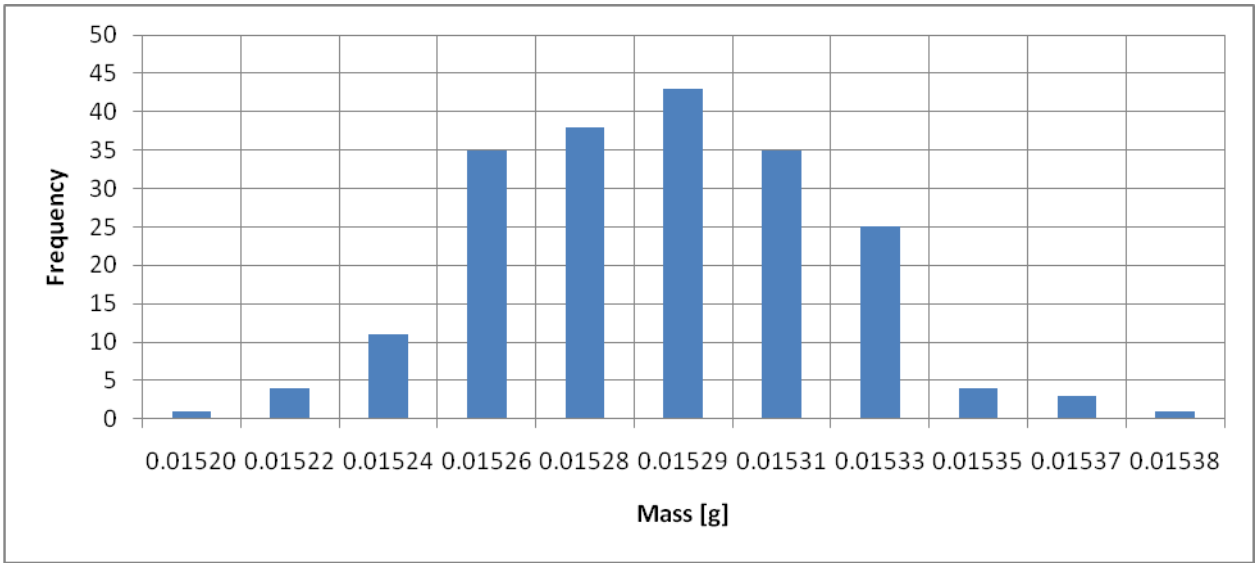

Figure 20. ^{135}I step 2 mass distribution.

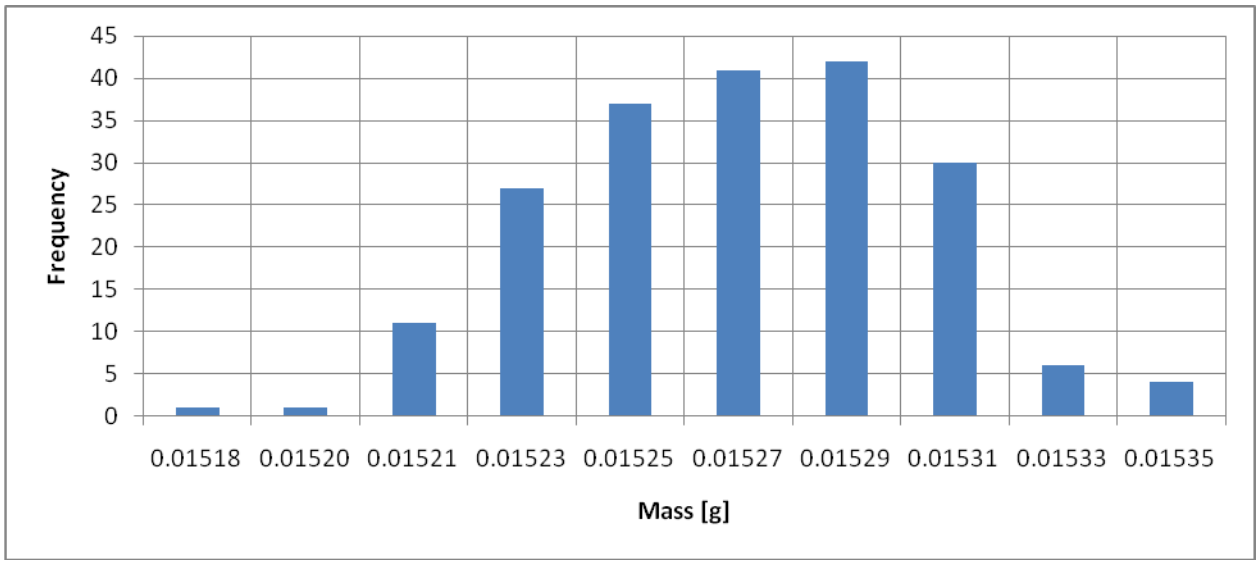

Figure 21. ^{135}I step 3 mass distribution.

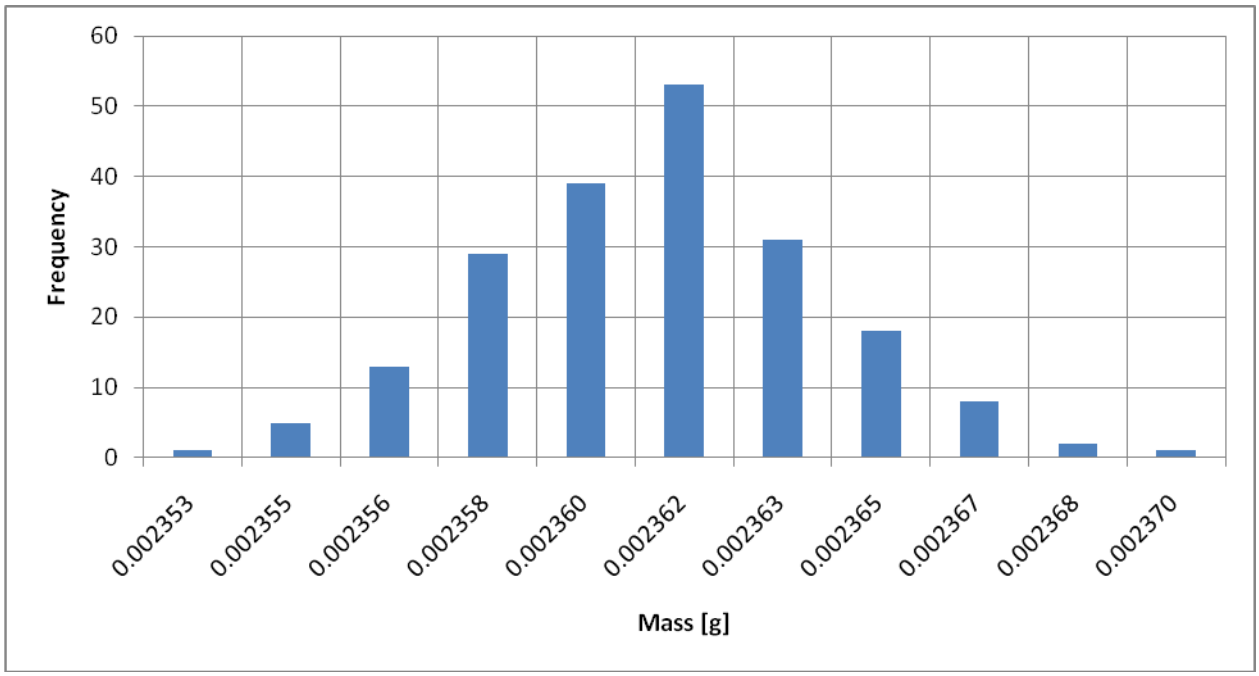

Figure 22. ^{135}Xe step 1 mass distribution.

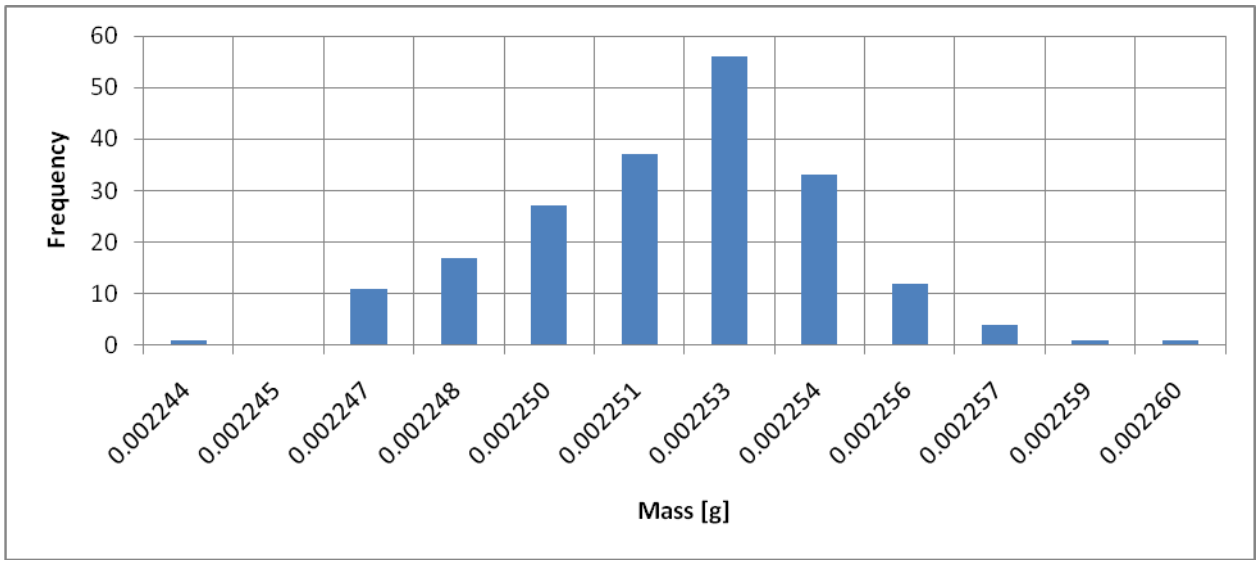

Figure 23. ^{135}Xe step 2 mass distribution.

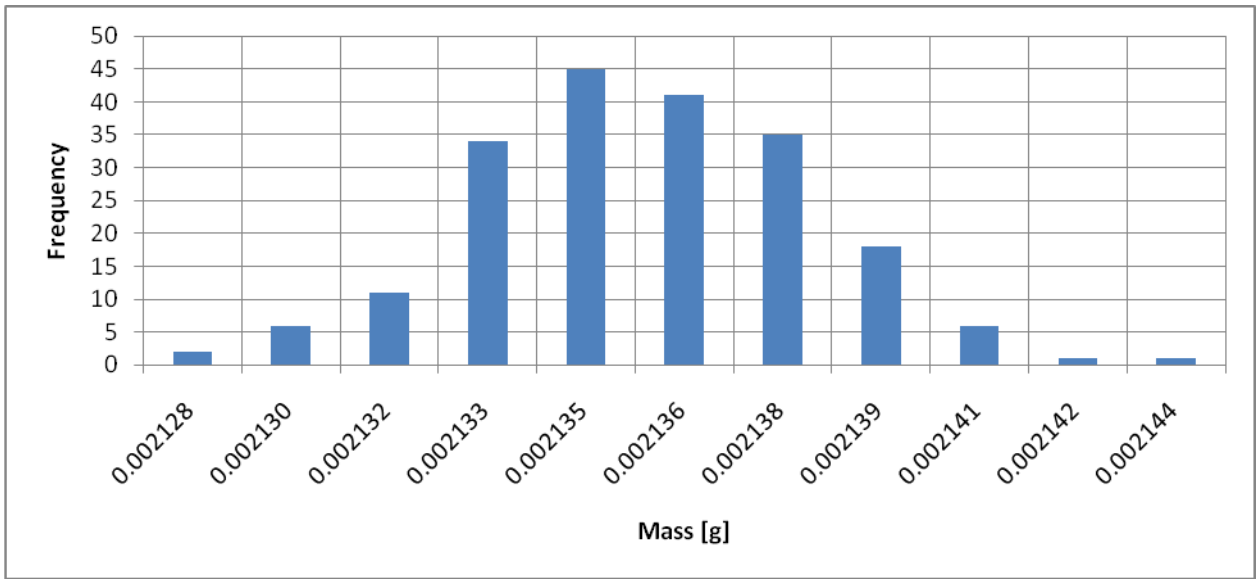

Figure 24. ^{135}Xe step 3 mass distribution.

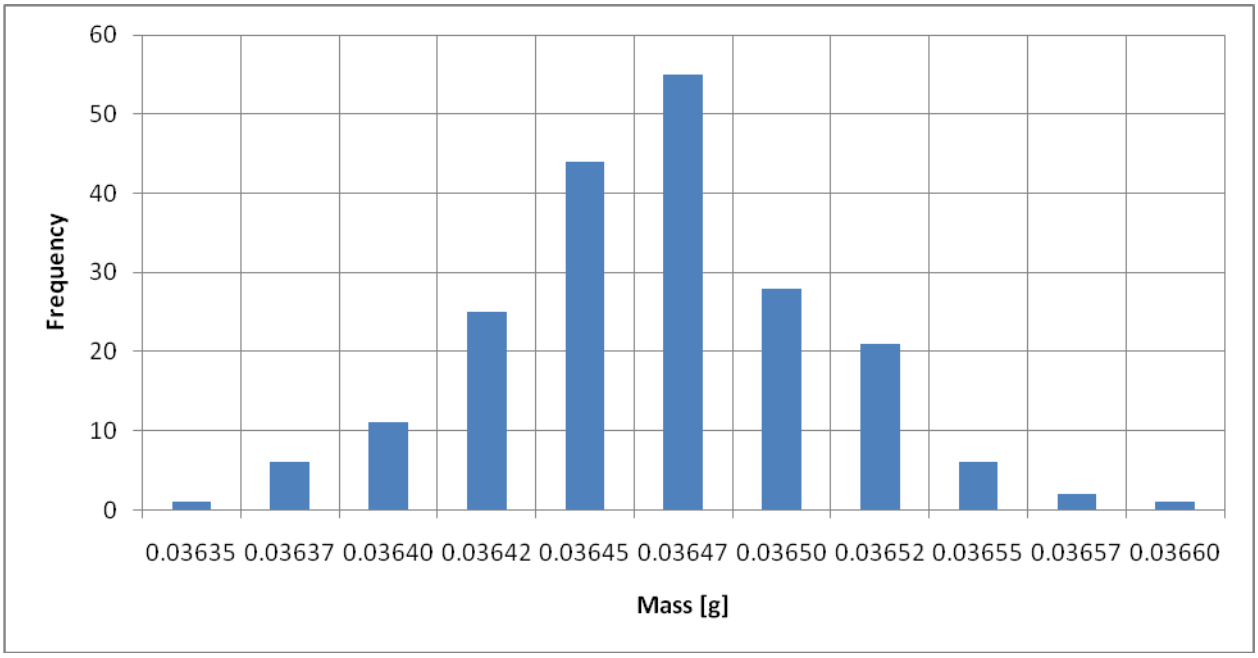

Figure 25. ^{135}Cs step 1 mass distribution.

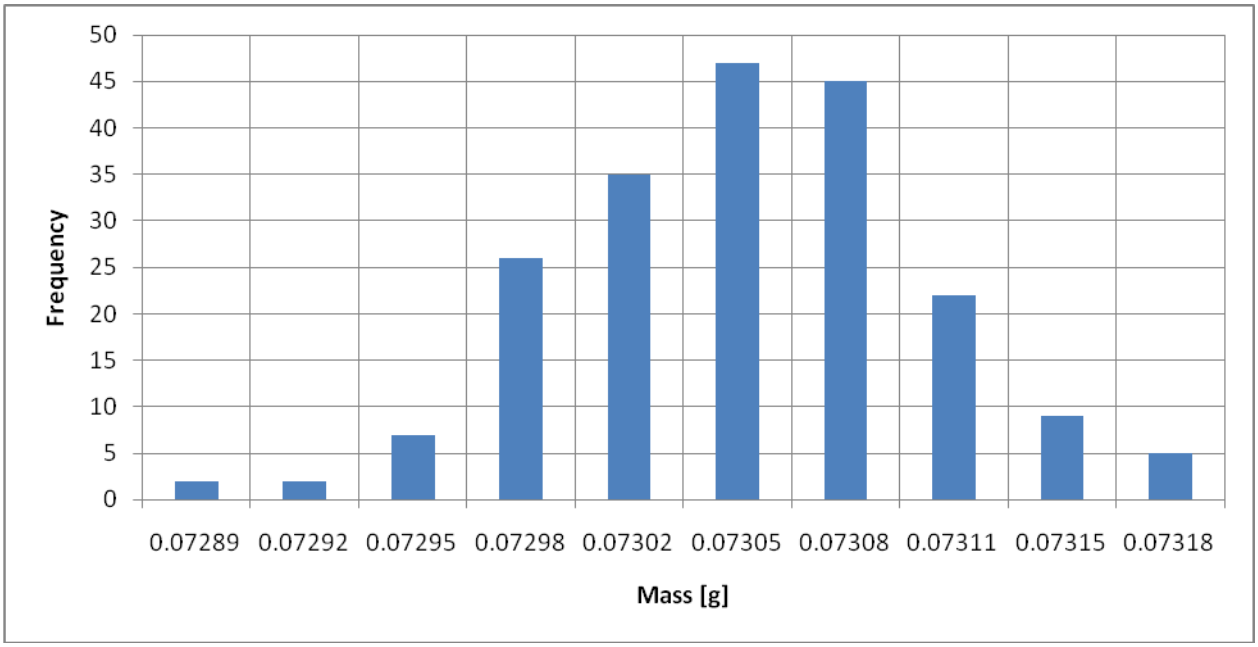

Figure 26. ^{135}Cs step 2 mass distribution.

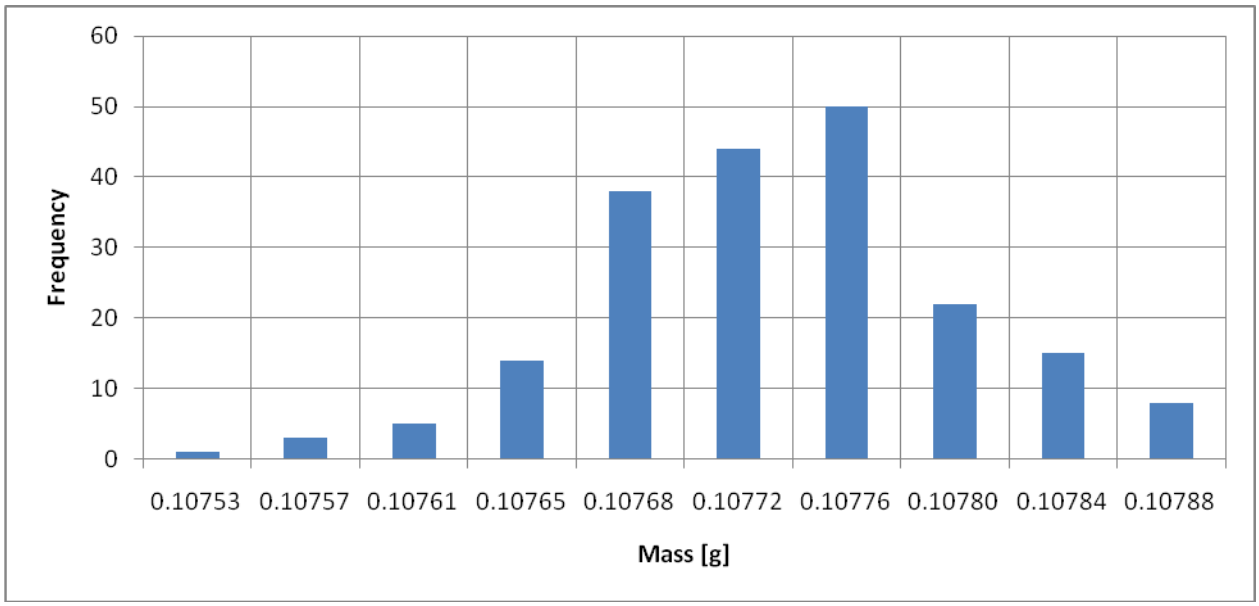

Figure 27. ^{135}Cs step 3 mass distribution.

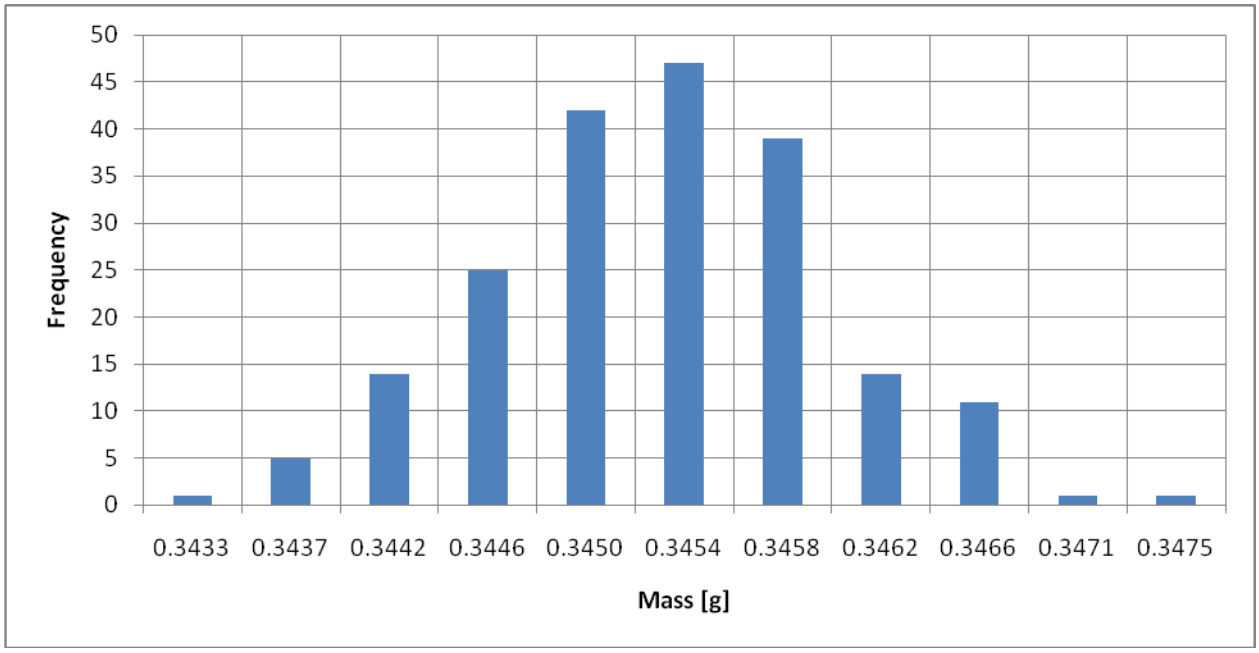

Figure 28. ^{137}Cs step 1 mass distribution.

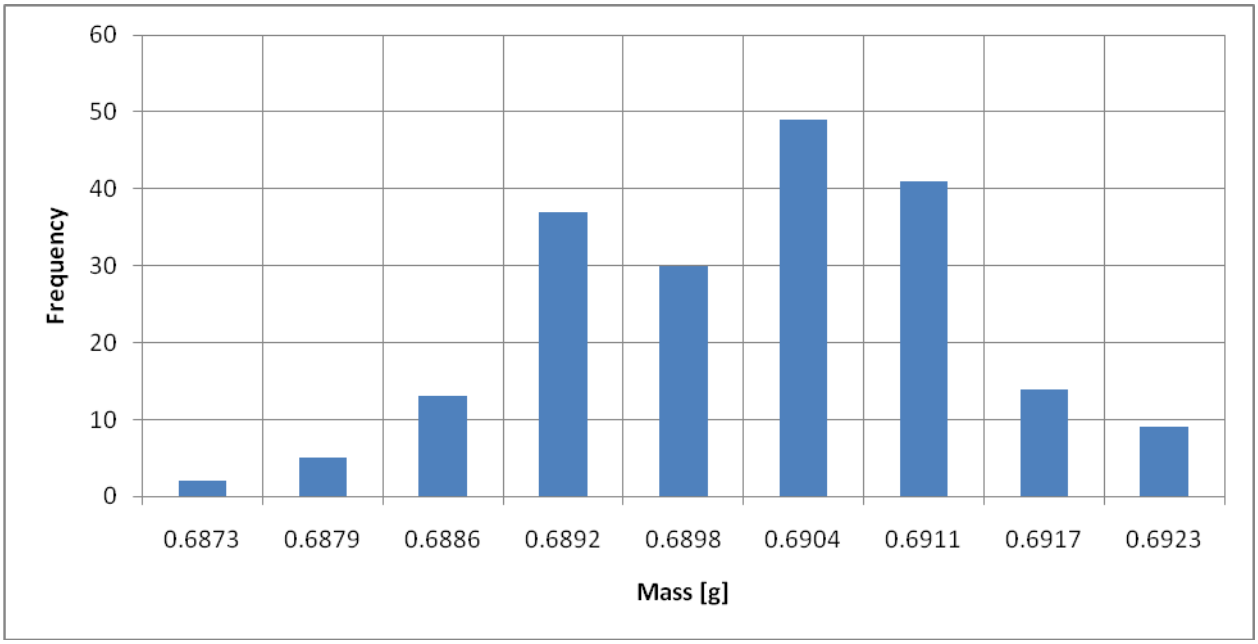

Figure 29. ^{137}Cs step 2 mass distribution.

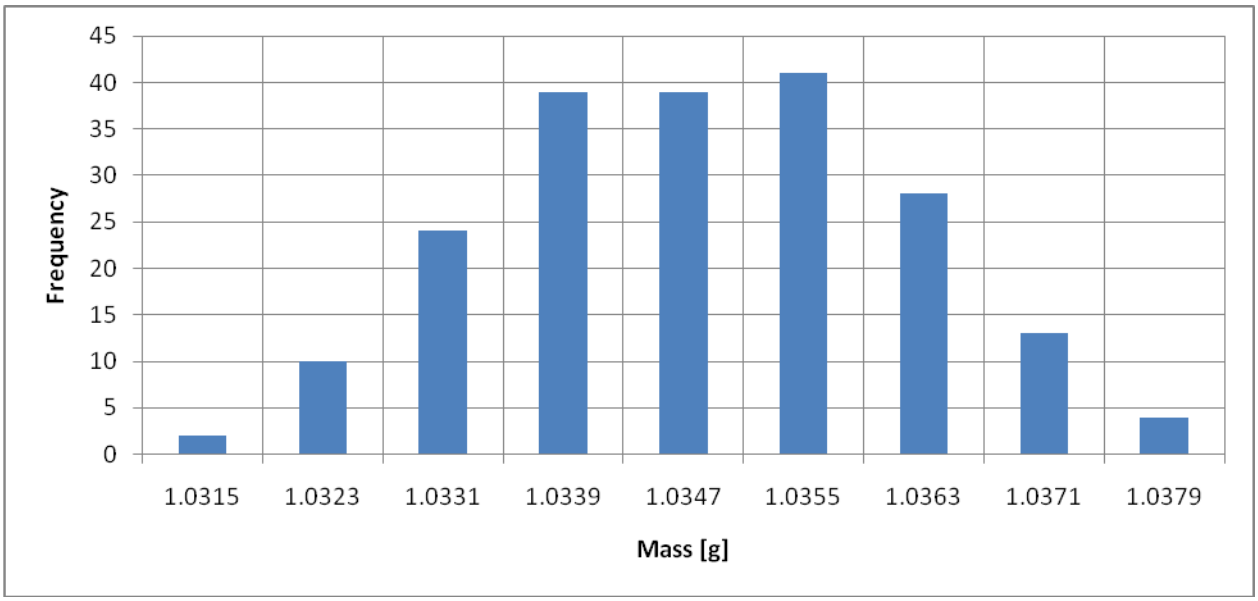

Figure 30. ^{137}Cs step 3 mass distribution.

APPENDIX D

Uranium isotope results figures.

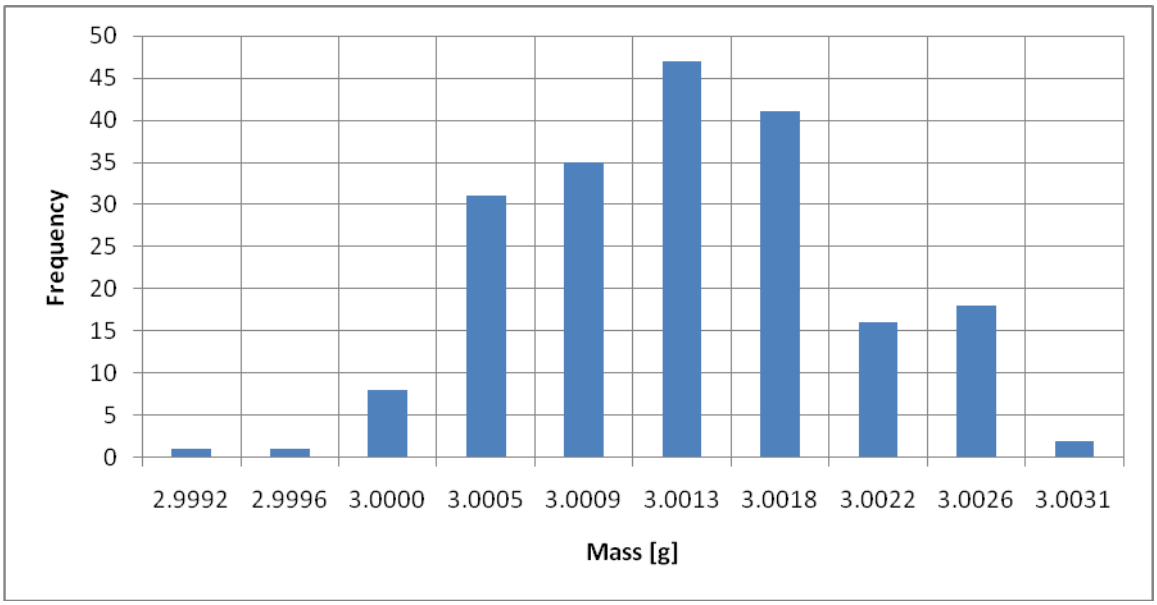

Figure 31. ^{234}U step 1 mass distribution.

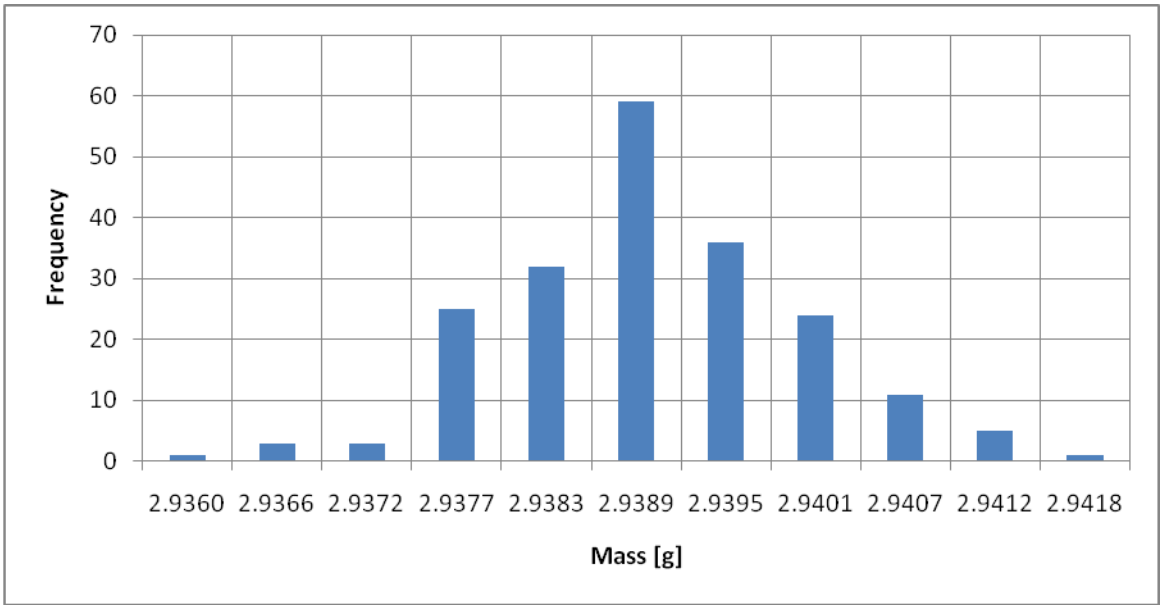

Figure 32. ^{234}U step 2 mass distribution.

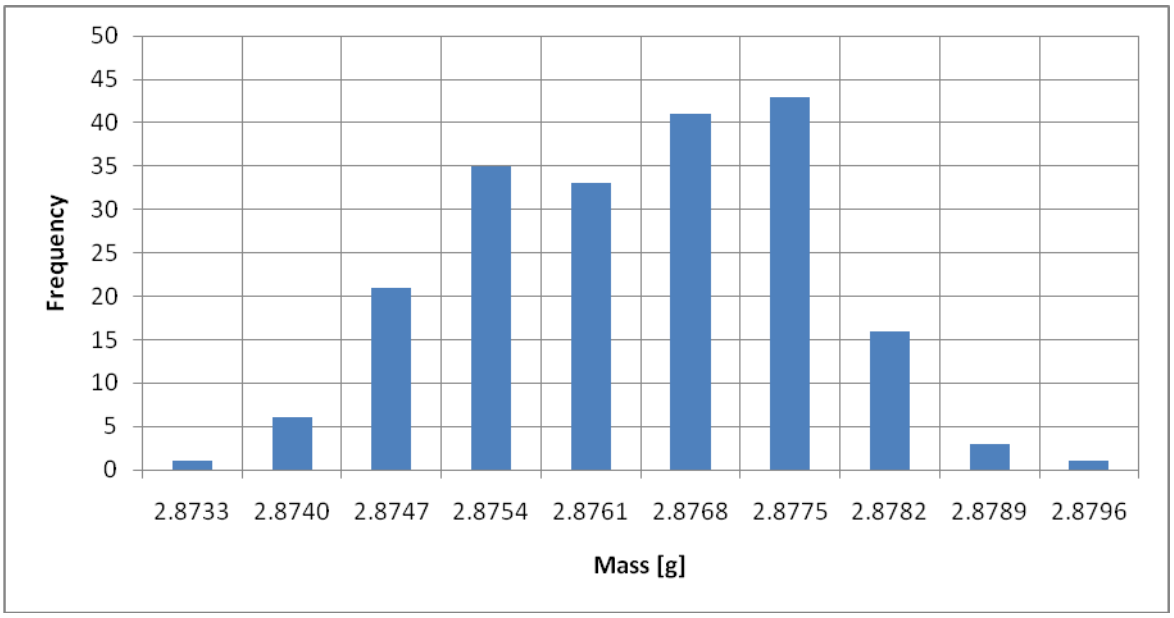

Figure 33. ^{234}U step 3 mass distribution.

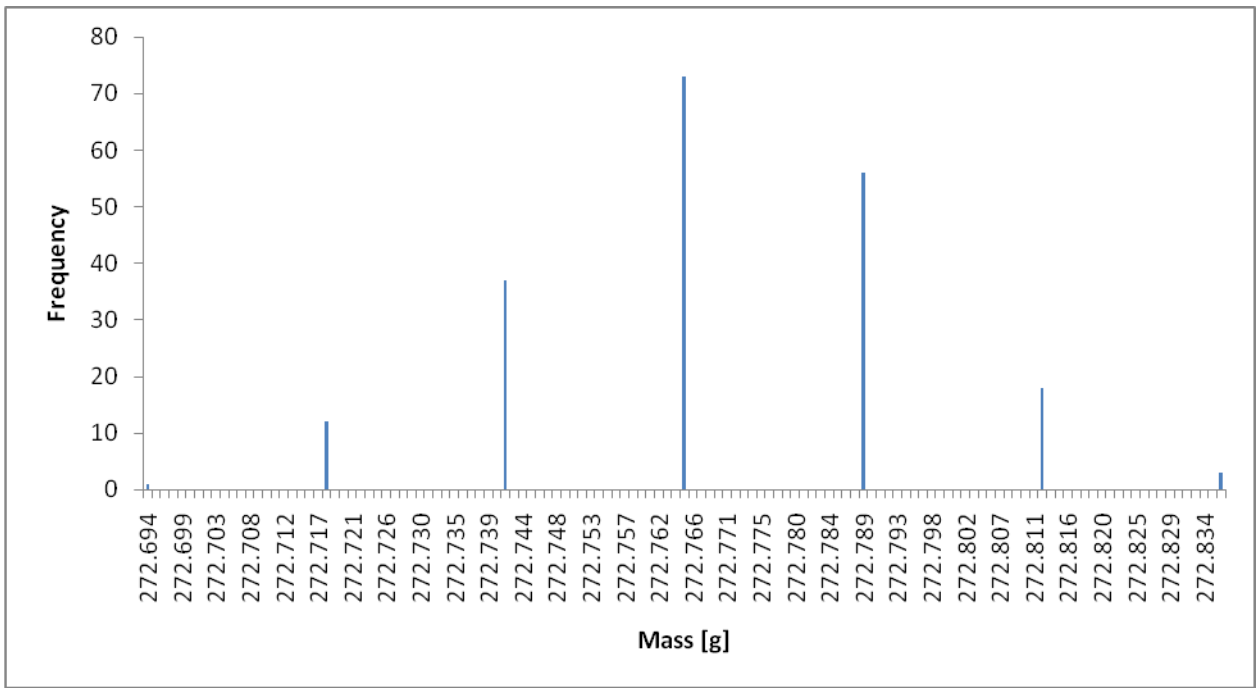

Figure 34. 100 bin histogram of ^{235}U step 1 mass data.

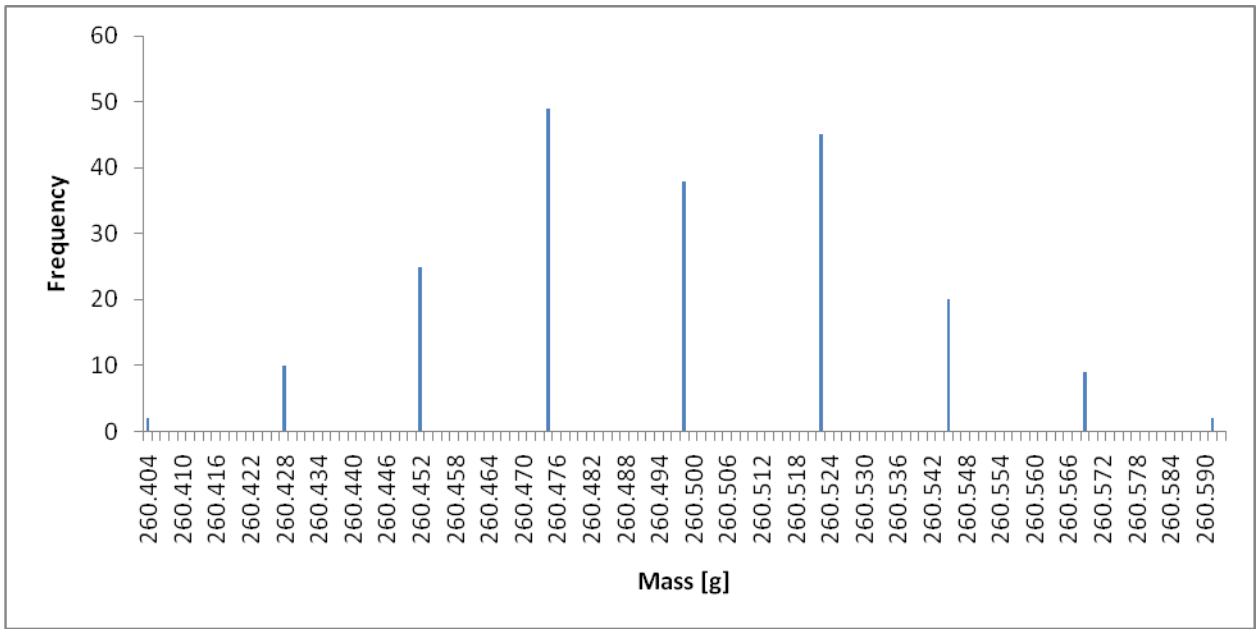

Figure 35. 100 bin histogram of ^{235}U step 2 mass data.

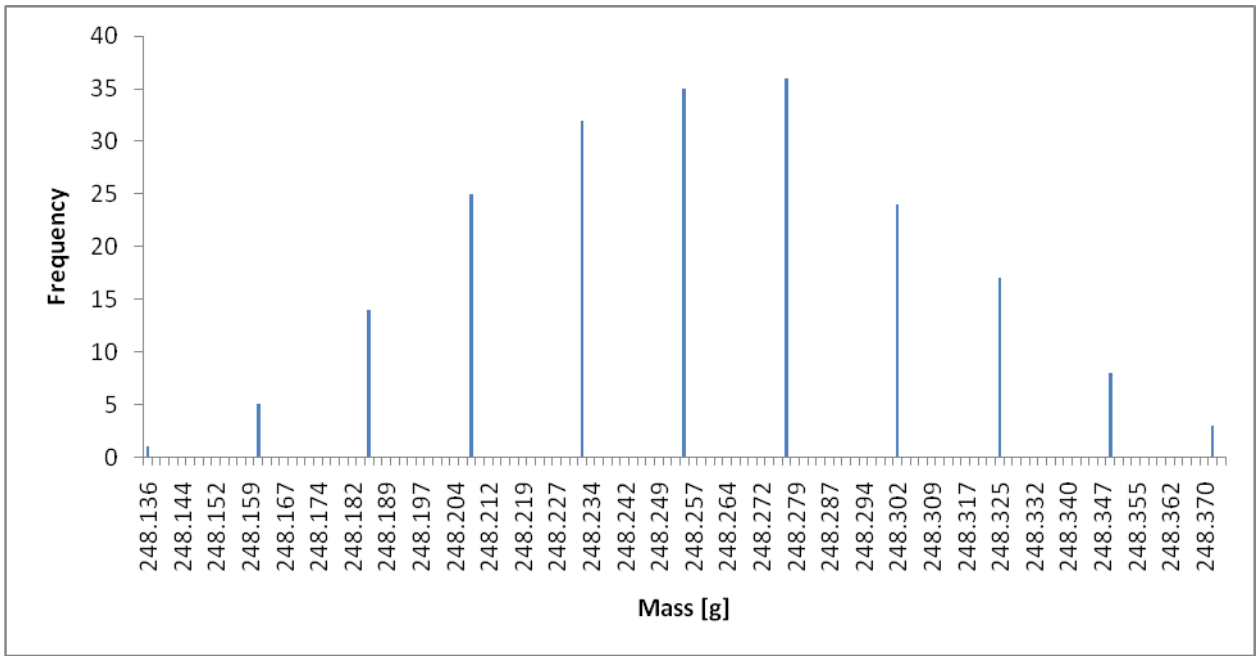

Figure 36. 100 bin histogram of ^{235}U step 3 mass data.

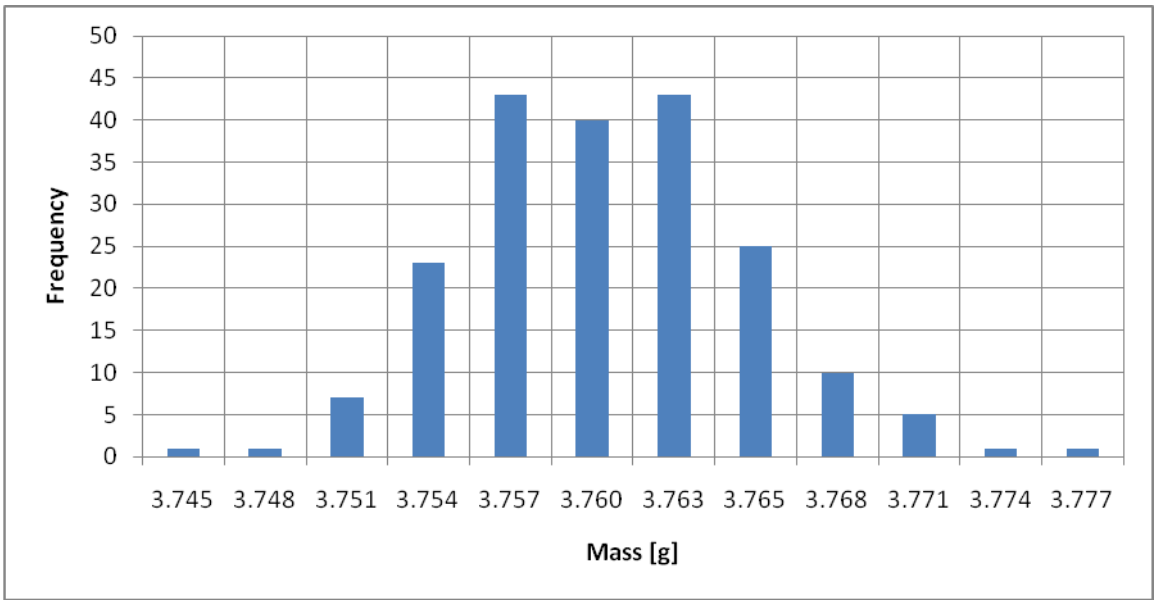

Figure 37. ^{236}U step 1 mass distribution.

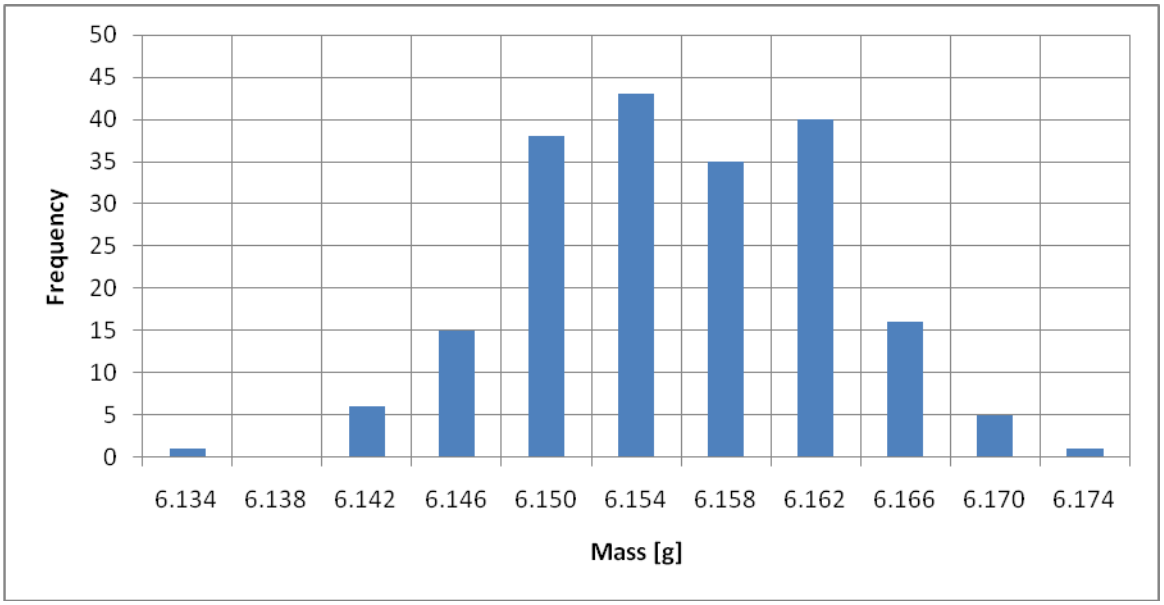

Figure 38. ^{236}U step 2 mass distribution.

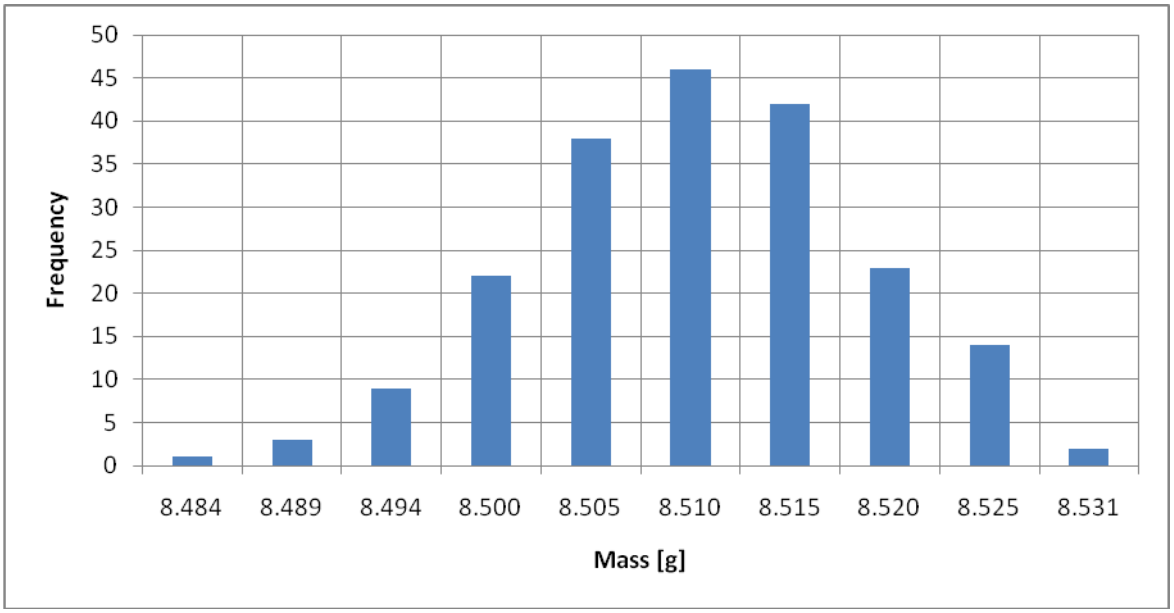

Figure 39. ^{236}U step 3 mass distribution.

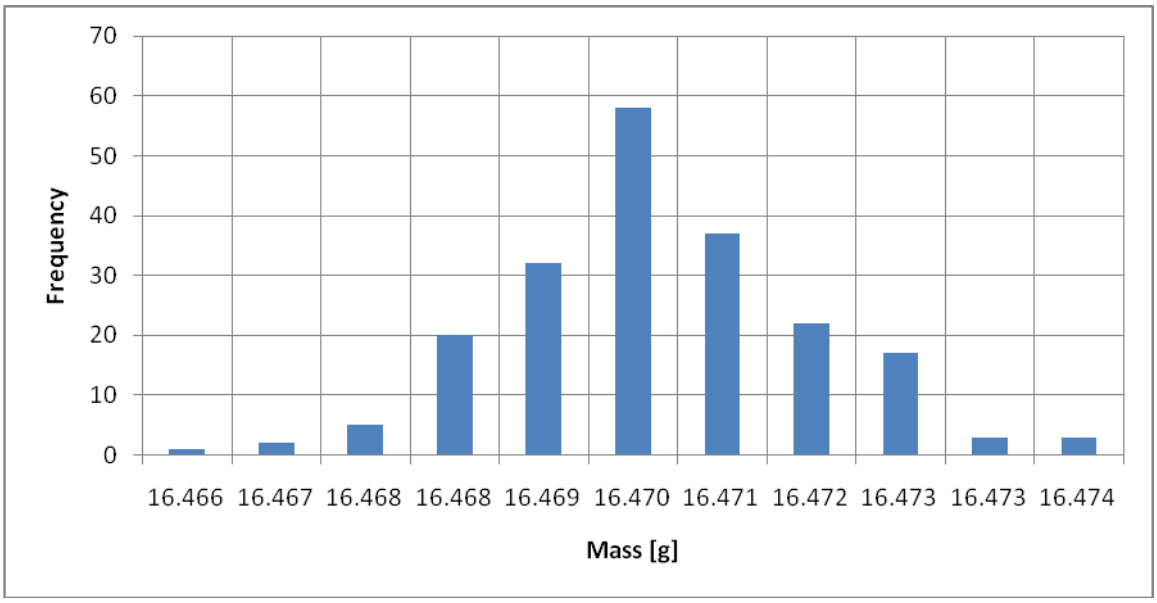

Figure 40. ^{238}U step 1 mass distribution.

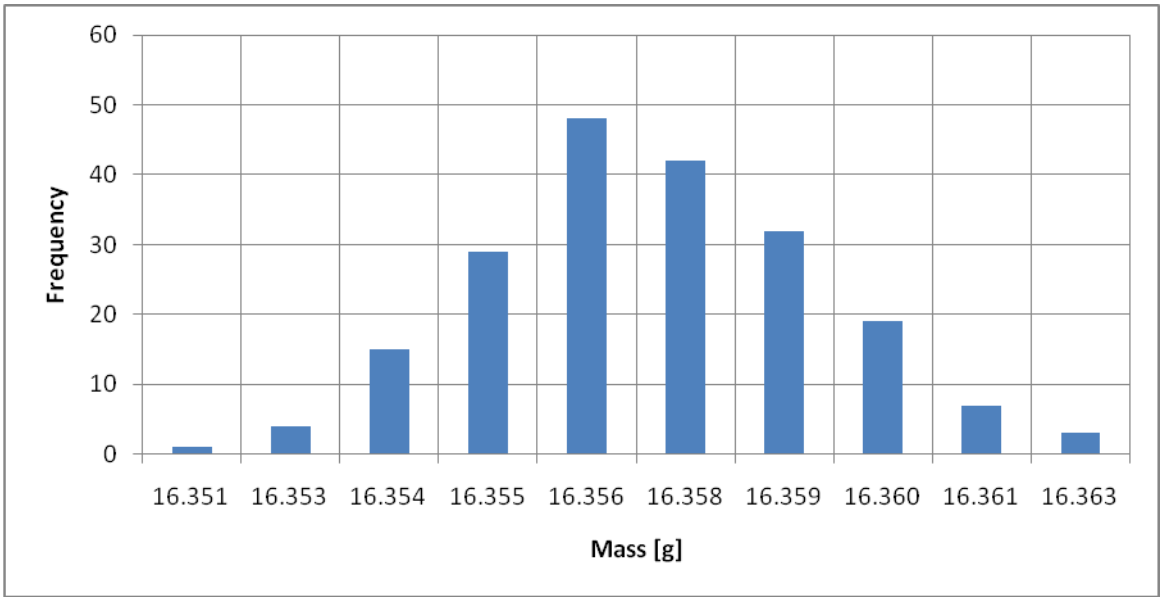

Figure 41. ^{238}U step 2 mass distribution.

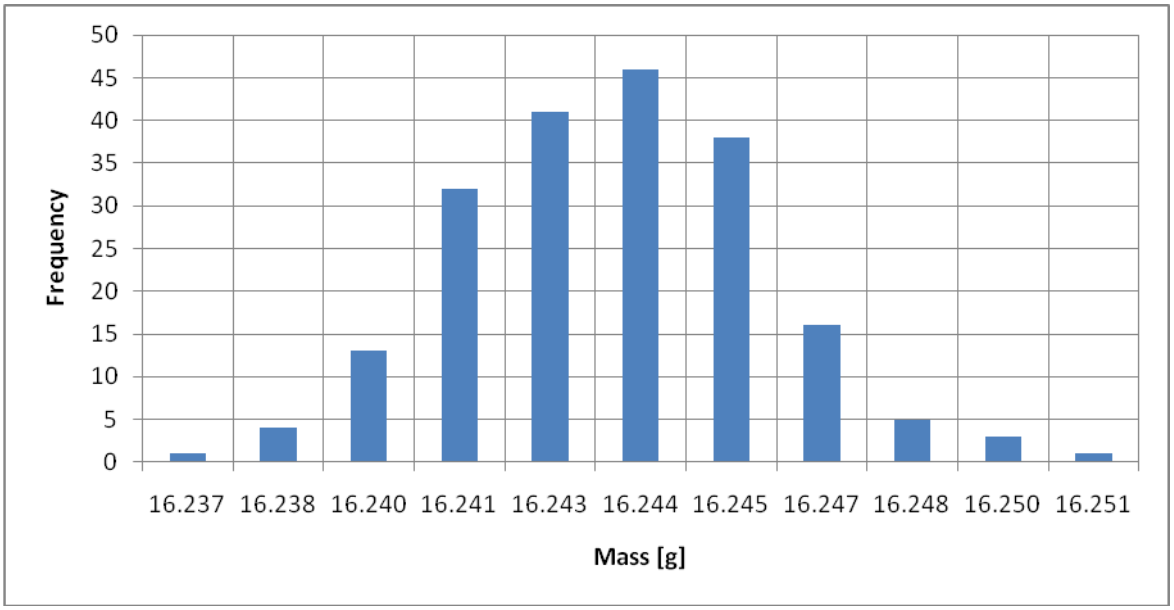

Figure 42. ^{238}U step 3 mass distribution.

APPENDIX E

MCNP k-effective detailed results.

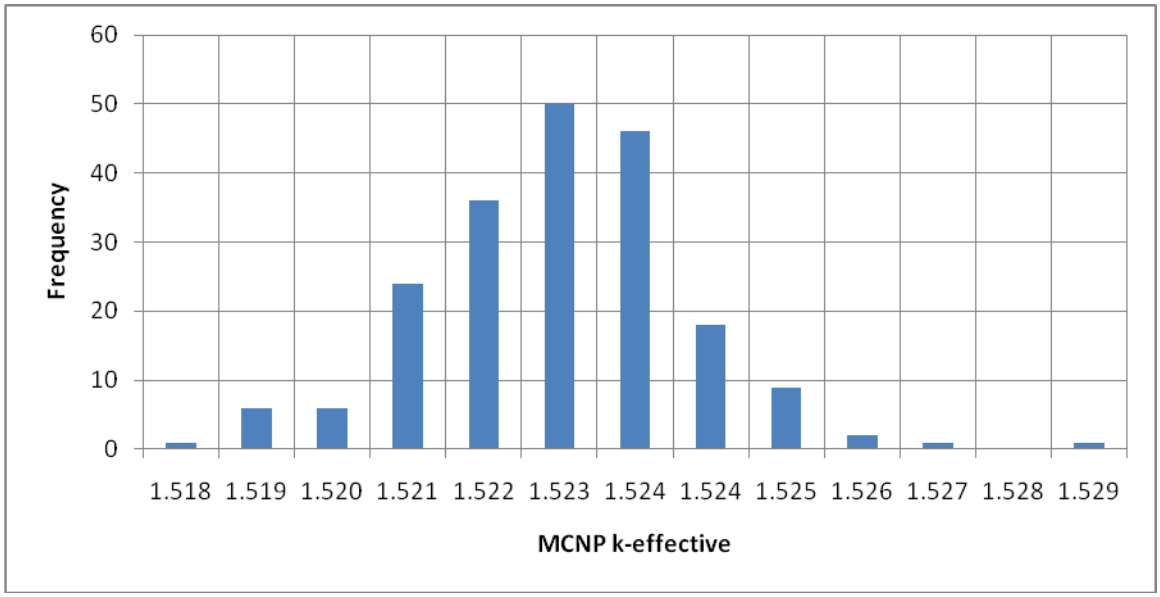

Figure 43. MCNP k-effective distribution at step 0.

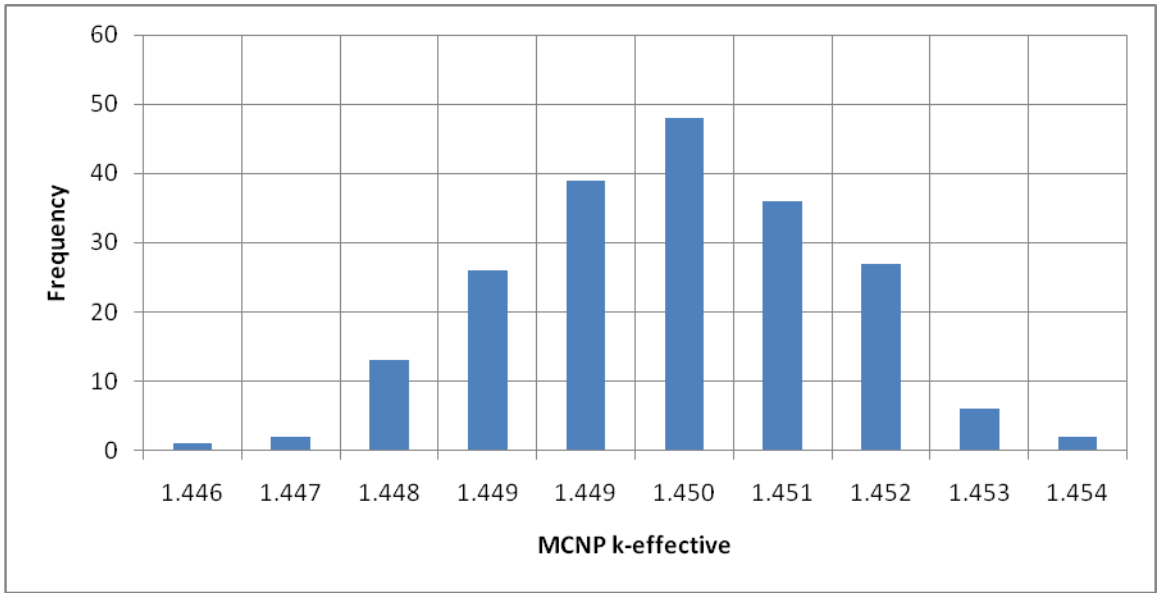

Figure 44. MCNP k-effective distribution at step 1.

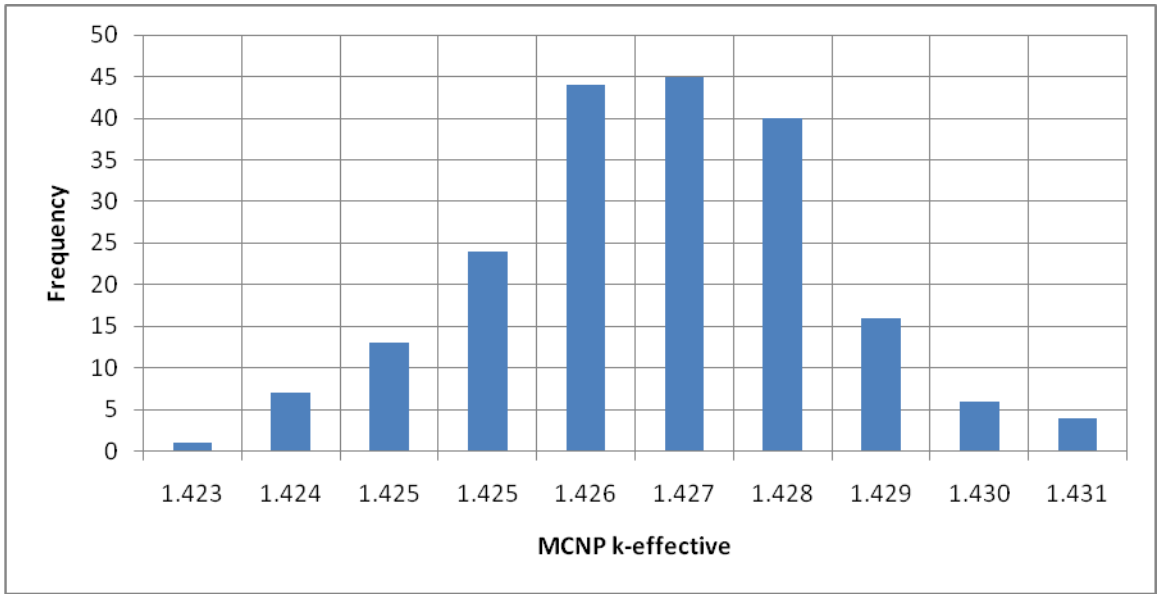

Figure 45. MCNP k-effective distribution at step 2.

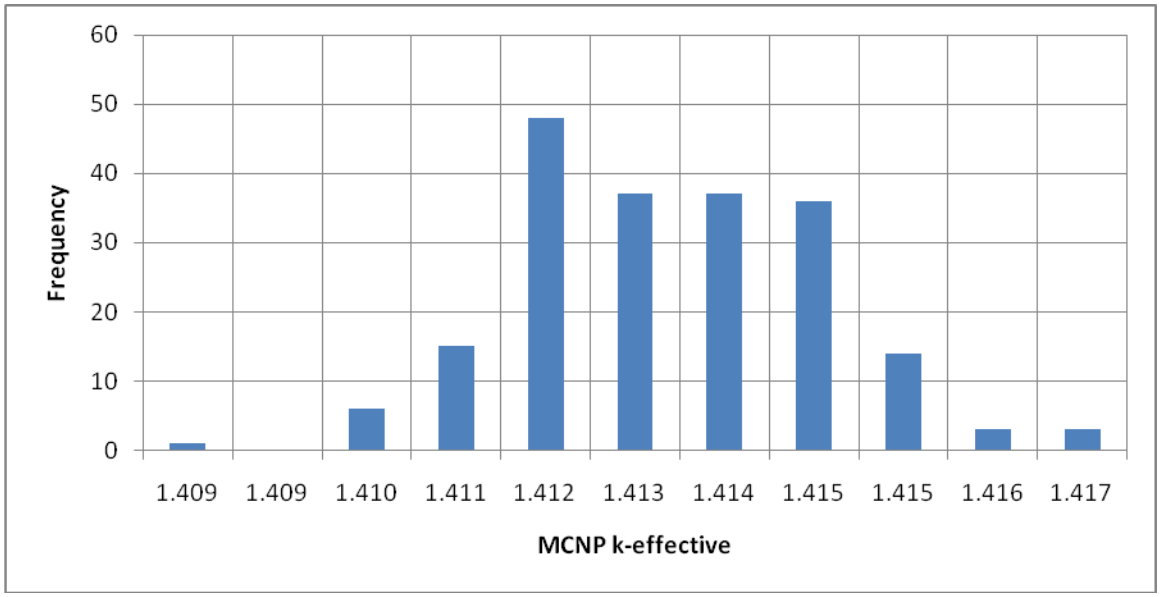

Figure 46. MCNP k-effective distribution at step 3.